Combination Chemotherapy Optimization with Discrete Dosing

Temitayo Ajayi, a Seyedmohammadhossein Hosseinian, b,* Andrew J. Schaefer, Clifton D. Fullerd

^a Nature Source Improved Plants, Ithaca, New York 14850; ^b Department of Mechanical and Materials Engineering, University of Cincinnati, Cincinnati, Ohio 45221; ^c Department of Computational Applied Mathematics and Operations Research, Rice University, Houston, Texas 77005; ^d Department of Radiation Oncology, The University of Texas MD Anderson Cancer Center, Houston, Texas 77030

Revised: April 22, 2023; August 26, 2023; September 8, 2023 Accepted: September 13, 2023

Received: July 11, 2022

Published Online in Articles in Advance: November 9, 2023

https://doi.org/10.1287/ijoc.2022.0207

Abstract. Chemotherapy drug administration is a complex problem that often requires expensive clinical trials to evaluate potential regimens; one way to alleviate this burden and better inform future trials is to build reliable models for drug administration. This paper presents a mixed-integer program for combination chemotherapy (utilization of multiple drugs) optimization that incorporates various important operational constraints and, besides dose and concentration limits, controls treatment toxicity based on its effect on the count of white blood cells. To address the uncertainty of tumor heterogeneity, we also propose chance constraints that guarantee reaching an operable tumor size with a high probability in a neoadjuvant setting. We present analytical results pertinent to the accuracy of the model in representing biological processes of chemotherapy and establish its potential for clinical applications through a numerical study of breast cancer.

History: Accepted by Paul Brooks, Area Editor for Applications in Biology, Medicine, & Healthcare. **Funding:** This work was supported by the National Science Foundation [Grants CMMI-1933369 and CMMI-1933373].

Supplemental Material: The software that supports the findings of this study is available within the paper and its Supplemental Information (https://pubsonline.informs.org/doi/suppl/10.1287/ijoc.2022.0207) as well as from the IJOC GitHub software repository (https://github.com/INFORMSJoC/2022.0207). The complete IJOC Software and Data Repository is available at https://informsjoc.github.io/.

Keywords: combination chemotherapy • differential equations • mixed-integer linear programming

1. Introduction

Chemotherapy is a prominent cancer treatment modality. In contrast to local treatment methods, such as surgery and radiation therapy, chemotherapy is a systemic treatment that targets cancer cells throughout the body. Hence, it is widely used for patients in advanced stages of cancer; more than 60% of the patients diagnosed with stage III or IV of breast, colon, rectal, lung, testicular, urinary bladder, and uterine corpus cancers in the United States underwent chemotherapy in 2016 (American Cancer Society 2021b). Chemotherapy drugs utilize cytotoxic as well as cytostatic agents. Cytotoxic drugs kill cancer cells, which results in tumor shrinkage; cytostatic drugs slow down the growth of malignant cells without killing them. The focus of this paper is on cytotoxic drugs. Because of their toxic nature and narrow therapeutic margin, cytotoxic drugs damage healthy cells as well and come with several, possibly life-threatening side effects (American Cancer Society 2021c). The main objective of chemotherapy planning is to determine administration dosage and schedule for these drugs such that a significant tumor shrinkage is achieved or, ideally, tumors disappear, while the adverse effects on healthy organs are minimized (American Cancer Society 2021c). Chemotherapy treatment plans are typically evaluated by randomized clinical trials (see, e.g., Ebata et al. 2018, Mariotti et al. 2021). Such trials are limited in variability because of constraints of permissible treatments and clinical and ethical considerations. Mathematical models of chemotherapy decisions can alleviate some of these burdens and aid treatment improvement and evaluation.

Mathematical models for chemotherapy planning must account for tumor evolution as well as the pharmacokinetics (distribution within the body) and pharmacodynamics (effect on tumor and healthy cells) of cytotoxic drugs. These processes take place in continuous time and are naturally described by ordinary differential equations (ODEs). In this regard, chemotherapy planning has been mainly approached as an optimal control (OC) problem in the literature. Swan and Vincent (1977) first studied chemotherapy planning as an OC problem, followed by the seminal models proposed by Martin et al. (1990) and Martin (1992); the objective of these models is to minimize the cancer cell population at the end of a treatment period subject to drug concentration limits—as a measure of toxicity—and intermediate tumor size or shrinkage rate. The early OC chemotherapy literature contains minimal details, which allows many of them to be solved analytical (these include Swan and Vincent 1977; Zietz and Nicolini 1979; Murray 1990, 1994; Panetta and Adam 1995; Murray 1997). Extending Martin et al. (1990) and Martin (1992), more complex and realistic OC models for chemotherapy optimization use approximation techniques (Martin et al. 1992a,b; Pereira et al. 1995; Costa and Boldrini 1997; de Pillis et al. 2007; Nanda et al. 2007; d'Onofrio et al. 2009; Harrold and Parker 2009; Itik et al. 2009) and heuristic algorithms (Iliadis and Barbolosi 2000, Tan et al. 2002, Floares et al. 2003, Villasana and Ochoa 2004, Liang et al. 2006, Tse et al. 2007, Alam et al. 2013). We refer to Shi et al. (2014) and Saville et al. (2019) for detailed surveys.

Continuous OC models capture the biological dynamics of chemotherapy processes well; however, cancer treatment involves important discrete components and operational constraints. For example, some cytotoxic drugs are available in the form of pills and are taken orally. For these drugs, an administration dose must be a multiple of the pill size, and any deviation from this regimen can lead to an underdose or overdose. Oral drugs are often prescribed to be taken with food, and metabolic processes can lead to mandated rest periods for certain drugs. These give a discrete nature to drug administration scheduling, which is not captured by continuous OC models. Modeling such operational constraints for chemotherapy planning requires integer control variables; introducing integer variables to OC models makes them extremely hard to solve, which poses a computational challenge to real-life applications (Sager 2005). In addition, the existing chemotherapy optimization models mainly impose treatment toxicity constraints implicitly through (fixed) limits on drug concentration. This presents another challenge to the applicability of these models to combination chemotherapy, that is, utilization of multiple drugs, which is the common practice in the presence of drug resistance (Luqmani 2005, Hu et al. 2016). In fact, in the absence of an explicit toxicity measure, these models do not clarify how the adverse effects of chemotherapy could vary under different combinations of administration regimens for multiple drugs.

Tumor heterogeneity is another important consideration in cancer treatment planning (Polyak 2011, Hu et al. 2017). Tumors are composed of different cell types with distinct characteristics; tumor heterogeneity is considered one of the main factors of therapeutic resistance (Cajal et al. 2020). Recent advances in next-generation sequencing technologies have made characterization of the cell composition of a tumor possible; this requires multiple, spatially separated samples from the tumor (Gerlinger et al. 2012, Piraino et al. 2019). The vast size of a tumor is the main barrier to complete characterization of the tumor composition; in a tumor with 109 cells (approximately 25 mm in diameter), the probability of sampling a genome that is present in 10⁵ cells is close to zero. Besides, invasive biopsies can lead to needle tract seeding, that is, implantation of cancerous cells in healthy regions, which may lead to cancer metastasis; a higher risk of seeding is incurred as the number of sampling passes increases (Tyagi and Dey 2014). In the absence of comprehensive samples, tumor heterogeneity remains uncertain for treatment planning (Abécassis et al. 2019). The only existing chemotherapy optimization models that consider this uncertainty include (Coldman and Goldie 1983, Day 1986, Coldman and Murray 2000). These models suffer from the same shortcomings as existing deterministic approaches. Moreover, they seek to maximize the probability of cure over the course of a treatment, which challenges their clinical relevance even more than the deterministic models. Finally, a similar problem to dose and schedule optimization in chemotherapy planning concerns finding an optimal sequence of therapies utilizing multiple drugs when each drug has a predetermined (fixed) regimen; we refer to He et al. (2016) and the references therein for more information on this line of research.

To fill the aforementioned gaps between the existing models of chemotherapy optimization and medical practice, we present a mixed-integer linear programming (MILP) model for combination chemotherapy planning, which seeks to find the optimal administration dose and schedule for cytotoxic drugs by minimizing the cancer cell population at the end of a treatment. We use discretization and linearization to recast ODEs representing the biological and pharmacological processes into an MILP framework; the flexibility of this framework allows for modeling complex operational constraints of chemotherapy. In particular, we incorporate discrete administration dose and schedule as well as clinically mandated rest periods in our model. We use the white blood cell count as an explicit measure of treatment toxicity. More specifically, we consider the effect of cytotoxic drugs on the count of two major white blood cell types, neutrophil and lymphocyte, which account for more than 80% of the total white blood cells. To address the uncertainty of tumor heterogeneity, we propose chance constraints and present a neoadjuvant (prior to a primary surgery) chemotherapy optimization model for treatment planning. We provide analytical results concerning the accuracy of the model in representing biological processes of chemotherapy. We use the clinical literature and published data for patients with breast cancer to calibrate our model parameters and perform sensitivity analysis to identify the most influential factors in a treatment outcome.

The structure of this paper is as follows: Section 2 presents chemotherapy modeling preliminaries, including tumor and white blood cell population dynamics, pharmacokinetics and pharmacodynamics of cytotoxic drugs, and operational constraints. Section 3 presents our deterministic and stochastic MILP models for combination chemotherapy planning along with our analytical results. Section 4 includes the model calibration details, and Section 5 describes our computational experiments. Section 6 concludes the paper. The proofs and some technical details are provided in the e-companion of the paper.

2. Modeling Preliminaries

Throughout this paper, we consider a treatment period $[0,T] \subset \mathbb{R}$ and a set of available cytotoxic drugs \mathcal{D} . For each drug $d \in \mathcal{D}$, the (continuous) functions $U_d(t)$ and $C_d(t)$ represent the administration dose and drug concentration, respectively, at time $t \in [0,T]$. We denote the set of cancer cell types by \mathcal{Q} , and for each cell type $q \in \mathcal{Q}$, we use $N_q(t)$ to represent the corresponding cell count as a function of time. We also introduce the variable functions $P_q(t) = \ln(N_q(t))$, $\forall q \in \mathcal{Q}$. Each cancer cell type is resistant to a (possibly empty) subset of drugs; drug resistance can be present even before chemotherapy starts (Swierniak et al. 2009). Finally, the white blood cell count at time $t \in [0,T]$ is denoted by $N_w(t)$; we distinguish between neutrophils and lymphocytes when we present the operational constraints of our models.

2.1. Cell Population Dynamics

Tumors proliferate by cell division and exhibit exponential growth in early stages, but the growth rate gradually decreases as malignant cells compete for limited nutritional resources. This resembles an S-curve growth, which is most commonly modeled by a Gompertzian function (e.g., Laird et al. 1965, Norton 1988, Harrold and Parker 2009, Frances et al. 2011, Tjørve and Tjørve 2017). The ODE representation of this function is

$$\dot{N}_q(t) = \Lambda N_q(t) \ln \left(\frac{\sum_{r \in \mathcal{Q}} N_{r,\infty}}{\sum_{r \in \mathcal{Q}} N_r(t)} \right), N_q(0) = N_{q,0}, \tag{1}$$

where $N_{q,0}$ is the initial population of a cancer cell type $q \in \mathcal{Q}$, $N_{r,\infty}$ denotes the steady-state (asymptotic) population limit for each cell type $r \in \mathcal{Q}$, and Λ is a shape parameter that dictates the rate at which the population transitions from the initial state to the steady-state limit.

The population dynamics of white blood cells are different. White blood cells are perpetually produced (mainly in bone marrow and the thymus gland) and circulate in the blood; they have a life span of a few days. Iliadis and Barbolosi (2000) model the white blood cell dynamics as follows:

$$\dot{N}_w(t) = v_w - v_w N_w(t), N_w(0) = N_{w,0}, \tag{2}$$

where v_w and v_w are the white blood cells' production and turnover rates, respectively, and $N_{w,0}$ denotes their (constant) level in the body under normal conditions. It is easy to verify that $N_w(t) = N_{w,0}$ is a solution to Equation (2) given $v_w = v_w N_{w,0}$.

Equations (1) and (2) provide the basis for our pharmacodynamics models.

2.2. Pharmacokinetics

A drug's distribution within the body (pharmacokinetics) is a complex, multicompartmental, and multiphase process. In cancer research, however, the dose profile of a cytotoxic drug is often represented by a single compartmental model, in which the drug concentration decays exponentially over time (Martin 1992, Jacqmin et al. 2007, Harrold and Parker 2009, Frances et al. 2011). The process is described by the following ODE:

$$\dot{C}_d(t) = -\xi_d C_d(t) + \frac{U_d(t)}{\mathscr{L}}, C_d(0) = 0, \tag{3}$$

where $\mathscr{V} > 0$ represents the volume of the "effect compartment" that is used to convert an administered dose to drug concentration and ξ_d is a constant characterizing the elimination rate of a drug $d \in \mathcal{D}$ in the body. In our models, the boundary condition $C_d(0) = 0$ indicates there is no drug in a patient's body before the start of treatment.

The underlying assumption of Equation (3) is that the contribution of a newly administered dose of a drug to its concentration profile starts from the peak it generates on the concentration curve. After a single administration, the drug concentration—time curve is highly right-skewed; it reaches its peak in a relatively short time, but it takes much longer for the drug to vanish. For the sake of simplicity, Equation (3) ignores the time it takes for a drug to reach its maximum concentration after administration.

2.3. Pharmacodynamics

The main paradigm of pharmacodynamics (drug effect) modeling in chemotherapy optimization is based on the seminal works of Skipper et al. (1964, 1967), which indicate that, given a dose of a cytotoxic drug, it kills a constant fraction of cancer cells. The fractional kill effect of a cytotoxic drug on cancer cells is modeled by adding a bilinear term composed of the product of drug concentration and cancer cell count with a constant factor to the cancer evolution model, that is, Equation (1). In combination chemotherapy, the effect of multiple drugs is commonly modeled following the additivity principal (see, e.g., Martin et al. 1992a, Petrovski et al. 2004, Tse et al. 2007, Frances et al. 2011). In an additive model, the drugs perform as if each acts in isolation, and the effects of all drugs are summed. The additivity assumption overlooks the possible interactions between different drugs to avoid interactability of the resultant models. Even though several combinations of chemotherapy drugs are shown to have synergistic effects (Wu et al. 2017, Tan et al. 2019, Nøhr-Nielsen et al. 2020), modeling such interactions accurately for every possible combination of drugs is very difficult. Our pharmacodynamics model follows Frances et al. (2011), who also assume an exponential decay on drug effectiveness over time because of the resistance developed in cancer cells when exposed to a drug, as follows:

$$\dot{N}_{q}(t) = \Lambda N_{q}(t) \ln \left(\frac{\sum_{r \in \mathcal{Q}} N_{r,\infty}}{\sum_{r \in \mathcal{Q}} N_{r}(t)} \right) - \sum_{d \in \mathcal{D}} \eta_{d,q} \exp(-\rho_{d,q} t) N_{q}(t) E_{d}(t), N_{q}(0) = N_{q,0}, \tag{4}$$

where $\eta_{d,q}$ is the fractional kill effect parameter of a drug $d \in \mathcal{D}$ on a cancer cell type $q \in \mathcal{Q}$, the parameter $\rho_{d,q}$ determines how drug effectiveness decays over time, and $E_d(t)$ denotes the effective concentration of a drug $d \in \mathcal{D}$ as a function of time. The effective concentration $E_d(t)$ indicates the amount that the drug concentration exceeds some threshold $\beta_{d,\text{eff}}$, below which the drug is ineffective therapeutically (Iliadis and Barbolosi 2000, Tan et al. 2002, Harrold and Parker 2009). By this definition,

$$E_d(t) = \max\{0, C_d(t) - \beta_{d, eff}\}.$$

With the logarithmic transformation $P_q(t) = \ln(N_q(t))$, $\forall q \in Q$, Equation (4) can be written as follows:

$$\dot{P}_{q}(t) = \Lambda \quad \ln \quad \sum_{r \in \mathcal{O}} N_{r,\infty} - \ln \quad \sum_{r \in \mathcal{O}} N_{r}(t) - \sum_{d \in \mathcal{D}} \eta_{d,q} \exp(-\rho_{d,q} t) E_{d}(t), P_{q}(0) = \ln(N_{q,0}). \tag{5}$$

The only nonlinearity of Equation (5) comes from the logarithmic term in Equation (4). Linear approximations of nonlinear ODEs are of great practical interest and huge computational benefit (He et al. 2016). An important property of the Gompertzian function (1) is that the growth rate at early stages of development is dominated by the exponential effect of $N_q(t)$; the logarithmic term becomes influential gradually as the population approaches the steady-state limit. Tumors are often diagnosed in relatively early stages, and without medical interventions, death happens way before the tumor reaches its natural carrying capacity (Norton 1988). This implies that the tumor (natural) growth model (1) can be generally approximated well by substituting its logarithmic term. In

particular, within an appropriate range of parameters, one may approximate $\frac{\sum_{r \in Q} N_{r,\infty}}{\sum_{r \in Q} N_{r}(t)}$ in (1) by $\frac{N_{q,\infty}}{N_{q}(t)}$ for cell type

 $q \in \mathcal{Q}$, where $N_{q,\infty}$ denotes the steady-state asymptotic limit of cell type q population. Such an approximation leads to the following linear ODE, which we use, in lieu of Equation (5), in our model:

$$\dot{P}_{q}(t) = \Lambda \left(\ln(N_{q,\infty}) - P_{q}(t) \right) - \sum_{d \in \mathcal{D}} \eta_{d,q} \exp(-\rho_{d,q} t) E_{d}(t), P_{q}(0) = \ln(N_{q,0}). \tag{6}$$

We verify the quality of this approximation for our case-study analysis of breast cancer later. Finally, we note that one may consider different shape parameters across the cell types; however, calibrating the parameter for individual cell types is impractical.

We model the fractional kill effect of cytotoxic drugs on white blood cells in a similar manner:

$$\dot{N}_{w}(t) = v_{w} - v_{w} N_{w}(t) - \sum_{d \in \mathcal{D}} \eta_{d,w} N_{w}(t) C_{d}(t - t_{w}), \ t \ge t_{w}, \tag{7}$$

where $\eta_{d,w}$ is the fractional kill effect parameter of a drug $d \in \mathcal{D}$ on white blood cells and t_w denotes the delay in the response of white blood cells to cytotoxic drugs (Iliadis and Barbolosi 2000). Note that, in Equation (7), we make conservative assumptions that white blood cells do not develop resistance to cytotoxic drugs over time, and the toxic effect of a drug exists even if its concentration is below the threshold $\beta_{d,\text{eff}}$. During the time interval $[0,t_w)$, the white blood cell population dynamics is governed by Equation (2).

2.4. Operational Constraints

Operational constraints enforce clinically permissible treatment plans. We consider a partition of the treatment period [0,T] into M days, each denoted by D_m , $m \in DAYS = \{1,...,M\}$. Because certain oral drugs are consumed with meals, three time points (periodic with respect to the days) are designated as meal times; this set of time points is denoted by MEALS.

We describe operational constraints captured by our model; some of these constraints are included in the chemotherapy optimization literature.

- 1. Maximum concentration (Martin et al. 1992a, Iliadis and Barbolosi 2000, Baker et al. 2006): For a drug $d \in \mathcal{D}$, let $\beta_{d,\text{conc}}$ denote the maximum permissible concentration in a patient's body; the corresponding constraint is $C_d(t) \leq \beta_{d,\text{conc}}, \ \forall t \in [0,T]$.
- 2. Maximum infusion rate (Hande 1998, Reigner et al. 2001, Baker et al. 2006, Ershler 2006, Palmeri et al. 2008): Let $\beta_{d,\text{rate}}$ denote the maximum permissible infusion rate for a drug $d \in \mathcal{D}$; the corresponding constraint is $U_d(t) \leq \beta_{d,\text{rate}}$, $\forall t \in [0,T]$.
- 3. Maximum daily cumulative dose (Hande 1998, Reigner et al. 2001, Baker et al. 2006, Ershler 2006, Palmeri et al. 2008): Clinical studies often seek to determine appropriate thresholds for drug administration within particular time periods. Daily cumulative dose constraints ensure that the administrated drugs in the model are reasonably close to tested protocols. Let $\beta_{d,\text{cum}}$ denote the maximum cumulative daily dose of a drug $d \in \mathcal{D}$; the corresponding constraint is $\int_{t \in D_m} U_d(t) dt \le \beta_{d,\text{cum}}$, $\forall m \in \text{DAYS}$.
- 4. Pill administration: Certain drugs are available via oral administration and, therefore, must be administered in discrete amounts (Hande 1998, Reigner et al. 2001, Ershler 2006, Sharma et al. 2006). These drugs are often recommended to be taken with food. For a drug $d \in \mathcal{D}$ that is available in an orally administered pill, let $\alpha_{d,\text{pill}}$ denote the pill's mass and the integer decision variable $Z_{d,\text{pill}}(t)$ be the number of pills administered at time t; we model this constraint as follows: $U_d(t) = \alpha_{d,\text{pill}} Z_{d,\text{pill}}(t)$, $Z_{d,\text{pill}}(t) \in \mathbb{Z}_+$, $\forall t \in \text{MEALS}$, and $U_d(t) = 0$, $\forall t \notin \text{MEALS}$.
- 5. Rest days (following treatment administration): Rest periods, in which no amount of a particular drug can be administered, may be mandatory clinically; see, for example, Baker et al. (2006). We introduce binary decision variables $Z_{d,\text{rest}}^m$ to indicate if a drug $d \in \mathcal{D}$ is not administered during day D_m . Given a mandated number of rest days $\alpha_{d,\text{rest}}$, we enforce this constraint by $\int_{t \in D_m} U_d(t) dt \le \beta_{d,\text{cum}} (1 Z_{d,\text{rest}}^m)$, $\sum_{l=0}^{\min\{\alpha_{d,\text{rest}}, M-m\}} (1 Z_{d,\text{rest}}^{m+l}) \le 1$, $Z_{d,\text{rest}}^m \in \mathbb{B}$, $\forall m \in \text{DAYS}$.
- 6. Toxicity: Drug toxicity is a major consideration in chemotherapy planning. We use the white blood cell count as a measure of toxicity and distinguish between neutrophil and lymphocyte, two major white blood cell types, which are responsible for different side effects, namely, neutropenia and lymphocytopenia, with different thresholds. Let $N_{\text{neu}}(t)$ and $N_{\text{lym}}(t)$ denote the count of neutrophils and lymphocytes, respectively, at time $t \in [0,T]$; we assume neutrophils and lymphocytes account for the fractions θ_{neu} and θ_{lym} of the total white blood cell count. The neutropenia and lymphocytopenia constraints are as follows: $N_{\text{neu}}(t) \ge \beta_{\text{neu}}$, $N_{\text{neu}}(t) = \theta_{\text{neu}} N_w(t)$, $\forall t \in [0,T]$, and $N_{\text{lym}}(t) \ge \beta_{\text{lym}}$, $N_{\text{lym}}(t) = \theta_{\text{lym}} N_w(t)$, $\forall t \in [0,T]$, where β_{neu} and β_{lym} are the clinical thresholds for neutropenia and lymphocytopenia, respectively.

We denote the set of treatment solutions satisfying the operational constraints by \mathcal{O} . As the neutropenia and lymphocytopenia constraints are operational, we also include the accompanying pharmacodynamics constraints, that is, Equations (2) and (7), within this set when we present our models.

3. Chemotherapy Optimization Models

The primary goal of chemotherapy is to reduce the number of cancer cells in the body. There are multiple ways to express this goal; one option is to focus on the end-of-treatment cell count. The objective of our model is to minimize $\sum_{q\in\mathcal{Q}}P_q(T)$, which is equivalent to minimizing the geometric mean of the cancer cell type populations at the end of the treatment period, that is, $(\prod_{q\in\mathcal{Q}}N_q(T))^{1/|\mathcal{Q}|}$. We note that one may prioritize cell types according

to their levels of malignancy by considering different coefficients for population variables in the objective function.

Based on the model components described in Section 2, the combination chemotherapy optimization problem can be formulated as follows:

$$\min \quad \sum_{q \in \mathcal{Q}} P_q(T) \tag{8a}$$

s.t.
$$\dot{C}_d(t) = -\xi_d C_d(t) + U_d(t)/\mathcal{V}, \quad \forall \ d \in \mathcal{D}, \ t \in [0, T],$$
 (8b)

$$C_d(0) = 0, \ \forall d \in \mathcal{D}, \tag{8c}$$

$$\dot{P}_q(t) = \Lambda \left(\ln(N_{q,\infty}) - P_q(t) \right) - \sum_{d \in \mathcal{D}} \eta_{d,q} \exp(-\rho_{d,q} t) E_d(t), \ \forall \, q \in \mathcal{Q}, \ t \in [0,T], \tag{8d}$$

$$P_q(0) = \ln(N_{q,0}), \quad \forall \, q \in \mathcal{Q}, \tag{8e}$$

$$E_d(t) = \max\{0, C_d(t) - \beta_{d, eff}\}, \ \forall d \in \mathcal{D}, \ t \in [0, T],$$
 (8f)

$$(\mathbf{U}(t), \mathbf{C}(t), N_{\text{neu}}(t), N_{\text{lym}}(t)) \in \mathcal{O}, \ \forall t \in [0, T],$$
(8g)

where $\mathbf{U}(t) = (U_1(t), \dots, U_{|\mathcal{D}|}(t))$ and $\mathbf{C}(t) = (C_1(t), \dots, C_{|\mathcal{D}|}(t))$ are the variable vectors representing drug administration and concentration, respectively. Nonegativity is enforced except for $P_q(t)$, $\forall q \in \mathcal{Q}$, which we consider a part of the definition of \mathcal{O} .

Formulation (8) is an OC problem involving discrete and continuous controls and nonlinear functions, which, given the scale of the instances arising in practice, is extremely hard to solve exactly. We use discretization and linearization techniques to approximate this problem by an MILP formulation, which is significantly more tractable. Harrold and Parker (2009) employ MILP to approximate an OC problem for single-drug chemotherapy optimization. Although their model does not consider several operational constraints, they show that this framework provides high-quality approximations for the pharmacokinetics and pharmacodynamics ODE models, that is, Equations (8b)–(8f), using two case studies. Here, we provide analytical results concerning the approximation quality of such a transformation. Through a case-study analysis of breast cancer, we also provide computational results confirming the quality of the employed approximations and the merit of the resultant MILP models for clinical applications.

In the rest of this section, we first present our MILP model for combination chemotherapy optimization, including details of the discretization and linearization techniques we use. We extend this model to address uncertainty in the heterogeneity of tumors and present a model for neoadjuvant chemotherapy planning under this uncertainty. Finally, we present our analytical results concerning the numerical stability and approximation quality of the proposed models.

3.1. MILP Model

To approximate the ODEs in (8), one may use Runge–Kutta (RK) methods as approximation schemes (Butcher 2007). We use (forward) Euler's method, that is, the first order RK method, which has been previously used in chemotherapy optimization (Harrold and Parker 2009). Given a (fixed) time step h, consider the discretization of the planning horizon [0,T] by S+1 points with the index set $S=\{0,\ldots,S\}$, where t(0)=0 and t(S)=T=Sh. The Euler's approximation of the pharmacokinetics model, that is, Equations (8b) and (8c), is as follows:

$$C_{d,s+1} = C_{d,s} - h \, \xi_d \, C_{d,s} + \frac{U_{d,s}}{\mathscr{V}}, \quad \forall \, d \in \mathcal{D}, \, s \in \{0, \dots, S-1\},$$

$$C_{d,0} = 0, \quad \forall \, d \in \mathcal{D}.$$
(9)

Note that, in Equation (8b), $U_d(t)$ represents the flux of a drug $d \in \mathcal{D}$, that is, dose administered per unit of time; setting the unit of time equal to h, $U_{d,s}$ denotes the dose administered at (discrete) time t(s). In (9), $C_{d,s}$ is the concentration of a drug $d \in \mathcal{D}$ at time t(s).

The pharmacodynamics model, that is, Equations (8d) and (8e), is approximated in a similar manner:

$$\begin{split} P_{q,s+1} &= P_{q,s} + h \Big(\Lambda \left(\ln(N_{q,\infty}) - P_{q,s} \right) - \sum_{d \in \mathcal{D}} \eta_{d,q} \exp(-\rho_{d,q} \, t(s)) \, E_{d,s} \Big), \ \, \forall \, q \in \mathcal{Q}, \, \, s \in \{0,\ldots,S-1\}, \\ P_{q,0} &= \ln(N_{q,0}), \ \, \forall \, q \in \mathcal{Q}, \end{split}$$

where $P_{q,s}$ denotes the logarithm of the population of cancer cell type $q \in \mathcal{Q}$ at time t(s).

Conventionally, the effective concentration constraints, that is, Equation (8f), are linearized by introducing auxiliary binary variables $Z_{E,d,s}$, $\forall d \in \mathcal{D}$, $s \in \{0, ..., S\}$, as follows:

$$\forall d \in \mathcal{D}, s \in \{0, \ldots, S\}$$
:

$$E_{d,s} \ge 0, \tag{10a}$$

$$E_{d,s} \ge C_{d,s} - \beta_{d,\text{eff}},\tag{10b}$$

$$E_{d,s} \le \beta_{d,conc} Z_{E,d,s}, \tag{10c}$$

$$E_{d,s} \le C_{d,s} - \beta_{d,eff} + \beta_{d,conc} (1 - Z_{E,d,s}),$$
 (10d)

$$Z_{E,d,s} \in \mathbb{B}$$
, (10e)

where $E_{d,s}$ is the effective concentration of a drug $d \in \mathcal{D}$ at time t(s); recall that $\beta_{d,\text{conc}}$ denotes the maximum permissible concentration for a drug $d \in \mathcal{D}$, that is, an upper bound on $C_{d,s}$, $\forall s \in \{0,\ldots,S\}$.

The discretization and linearization of operational constraints are straightforward except for the white blood cell population dynamics model, that is, Equation (7). We present our model for the white blood cell population dynamics here and provide the details of other operational constraints in the e-companion; see Online Appendix A.

Applying Euler's method to Equation (7) results in the following discretization of the white blood cell population dynamics model:

$$N_{w,s+1} = N_{w,s} + h \quad v_w - v_w N_{w,s} - \sum_{d \in \mathcal{D}} \eta_{d,w} N_{w,s} C_{d,s-\tau} , \quad \forall s \in \{\tau, \dots, S-1\},$$
(11)

where $N_{w,s}$ denotes the total white blood cell count at time t(s) and τ corresponds to the time delay t_w in the ODE model. To address the bilinearity of Equation (11), we consider two approaches: McCormick relaxation and discretization. In the first approach, we replace each bilinear term $N_{w,s}C_{d,s-\tau}$ in (11) with a new variable $B_{d,s}$ and add the corresponding McCormick envelopes (McCormick 1976, Al-Khayyal and Falk 1983) to the formulation. Recall that $C_{d,s-\tau} \in [0,\beta_{d,\mathrm{conc}}]$. We also assume $N_{w,s} \in [\beta_w,N_{w,0}]$, where β_w is a lower bound on the white blood cell count that can be easily obtained from the clinical bounds on the neutrophil and lymphocyte counts, that is, $\beta_w = \min \left\{ \frac{\beta_{\mathrm{neu}}}{\theta_{\mathrm{neu}}}, \frac{\beta_{\mathrm{lym}}}{\theta_{\mathrm{lym}}} \right\}$ and $N_{w,0}$ denotes the initial count of white blood cells that serves as an upper bound on the white blood cell count during the treatment period. The white blood cell count is discrete, but the continuity assumption is not far from the reality given the magnitude of this quantity, that is, $O(10^9)$ cells per liter. The McCormick relaxation of Equation (11) is as follows:

$$N_{w,s+1} = N_{w,s} + h \quad v_w - v_w N_{w,s} - \sum_{d \in \mathcal{D}} \eta_{d,w} B_{d,s} , \quad \forall s \in \{\tau, \dots, S-1\},$$
 (12a)

$$B_{d,s} \ge \beta_w C_{d,s-\tau}, \ \forall d \in \mathcal{D}, \ s \in \{\tau, \dots, S-1\}, \tag{12b}$$

$$B_{d,s} \ge N_{w,0} C_{d,s-\tau} + \beta_{d,\text{conc}} N_{w,s} - N_{w,0} \beta_{d,\text{conc}}, \ \forall d \in \mathcal{D}, \ s \in \{\tau, \dots, S-1\},$$
 (12c)

$$B_{d,s} \le N_{w,0} C_{d,s-\tau}, \ \forall d \in \mathcal{D}, \ s \in \{\tau, \dots, S-1\},$$
 (12d)

$$B_{d,s} \le \beta_w C_{d,s-\tau} + \beta_{d,\operatorname{conc}} N_{w,s} - \beta_w \beta_{d,\operatorname{conc}}, \ \forall \ d \in \mathcal{D}, \ s \in \{\tau, \dots, S-1\}.$$

The drawback of the continuous McCormick relaxation is that the approximation quality of the bilinear sum is not controllable. Therefore, we also consider a modified form of the discretization approach proposed by Gupte et al. (2013); given the scale of approximated variables, we alter the constraints provided in this work. As a factor in the bilinear terms, the white blood cell count is approximated by discrete variables within some specified value Δ of maximum error. We introduce auxiliary binary variables $Z_{w,s,k}$, $\forall k \in \{0,\ldots,K\}$, which select the approximations of $N_{w,s}$, and continuous variables $V_{d,s,k}$, $\forall k \in \{0,\ldots,K\}$, which mirror the value of $C_{d,s-\tau}$.

Following Gupte et al. (2013), the approximation of Equation (11) is as follows:

$$N_{w,s+1} = N_{w,s} + h \quad v_w - v_w N_{w,s} - \sum_{d \in \mathcal{D}} \eta_{d,w} B_{d,s} , \quad \forall s \in \{\tau, \dots, S-1\},$$
 (13a)

$$N_{w,s} - \beta_w + \sum_{k=1}^K k \Delta Z_{w,s,k} \le \frac{\Delta}{2}, \ \forall s \in \{\tau, \dots, S-1\},$$
 (13b)

$$-N_{w,s} + \beta_w + \sum_{k=1}^K k \Delta Z_{w,s,k} \le \frac{\Delta}{2}, \ \forall s \in \{\tau, \dots, S-1\},$$
 (13c)

$$\sum_{k=0}^{K} Z_{w,s,k} = 1, \ \forall s \in \{\tau, \dots, S-1\},\tag{13d}$$

$$B_{d,s} = \sum_{k=1}^{K} (\beta_w + k\Delta) V_{d,s,k}, \ \forall d \in \mathcal{D}, \ s \in \{\tau, \dots, S - 1\},$$
 (13e)

$$V_{d,s,k} \le \beta_{d,\text{conc}} Z_{w,s,k}, \ \forall d \in \mathcal{D}, \ s \in \{\tau, \dots, S-1\}, \ k \in \{1, \dots, K\},$$
 (13f)

$$V_{d,s,k} \le C_{d,s-\tau}, \ \forall \ d \in \mathcal{D}, \ s \in \{\tau, \dots, S-1\}, \ k \in \{1, \dots, K\},$$
 (13g)

$$V_{d,s,k} \ge C_{d,s-\tau} + \beta_{d,\text{conc}}(Z_{w,s,k} - 1), \ \forall d \in \mathcal{D}, \ s \in \{\tau, \dots, S - 1\}, \ k \in \{1, \dots, K\},$$
 (13h)

$$V_{d,s,k} \ge 0, \ \forall d \in \mathcal{D}, \ s \in \{\tau, \dots, S-1\}, \ k \in \{1, \dots, K\},$$
 (13i)

$$Z_{w,s,k} \in \mathbb{B}, \ \forall s \in \{\tau, \dots, S-1\}, \ k \in \{1, \dots, K\}.$$
 (13j)

In (13), the quantity $\beta_w + \sum_{k=1}^K k \Delta Z_{w,s,k}$ approximates the value of $N_{w,s}$; the variable $V_{d,s,k}$ equals $C_{d,s-\tau}$ if and only if $Z_{w,s,k} = 1$ (0 otherwise), and $B_{d,s}$ approximates the bilinear term $N_{w,s}C_{d,s-\tau}$.

Before the effect of drugs on white blood cells starts, that is, $\forall s \in \{0, ..., \tau - 1\}$, we have $N_{w,s+1} = N_{w,s} + h(v_w - v_w N_{w,s})$, where $N_{w,0}$ equals the count of white blood cells before treatment. The discretized neutropenia and lymphocytopenia constraints are as follows: $N_{\text{neu},s} \ge \beta_{\text{neu}}$, $N_{\text{neu},s} = \theta_{\text{neu}} N_{w,s}$, $\forall s \in \{0, ..., S\}$, and $N_{\text{lym},s} \ge \beta_{\text{lym}}$, $N_{\text{lym},s} = \theta_{\text{lym}} N_{w,s}$, $\forall s \in \{0, ..., S\}$.

Formulation (14) presents our MILP model for combination chemotherapy optimization as the result of described discretization and linearization techniques applied to (8). In this formulation, we use $\hat{\mathcal{O}}$ to denote the set of treatment solutions satisfying the discretized operational constraints, including the constraint sets (12) or (13).

$$\min \sum_{q \in \mathcal{Q}} P_{q,S} \tag{14a}$$

s.t.
$$C_{d,s+1} = C_{d,s} - h \, \xi_d \, C_{d,s} + U_{d,s} / \mathcal{V}, \quad \forall \, d \in \mathcal{D}, \, s \in \{0, \dots, S-1\},$$
 (14b)

$$C_{d,0} = 0, \ \forall d \in \mathcal{D}, \tag{14c}$$

$$P_{q,s+1} = P_{q,s} + h \left(\Lambda (\ln(N_{q,\infty}) - P_{q,s}) - \sum_{d \in \mathcal{D}} \eta_{d,q} \exp(-\rho_{d,q} t(s)) E_{d,s} \right),$$

$$\forall q \in \mathcal{Q}, \ s \in \{0, \dots, S-1\},$$
(14d)

$$P_{a,0} = \ln(N_{a,0}), \ \forall a \in \mathcal{Q}, \tag{14e}$$

$$(10a) - (10e), \ \forall d \in \mathcal{D}, \ s \in \{0, \dots, S\},$$
 (14f)

$$(\mathbf{U}, \mathbf{C}, \mathbf{N}_{\text{neu}}, \mathbf{N}_{\text{lym}}) \in \hat{\mathcal{O}}, \tag{14g}$$

where $\mathbf{U} = [U_{d,s}, d \in \mathcal{D}, s \in \mathcal{S}]$ and $\mathbf{C} = [C_{d,s}, d \in \mathcal{D}, s \in \mathcal{S}]$ are the variable matrices representing drug administration and concentration, respectively, and $\mathbf{N}_{\text{neu}} = (N_{\text{neu},0}, \dots, N_{\text{neu},S})$ and $\mathbf{N}_{\text{lym}} = (N_{\text{lym},0}, \dots, N_{\text{lym},S})$ are the variable vectors of the neutrophil and lymphocyte count, respectively. Equations (14b) and (14c) are the discretized pharmacokinetics model (see (8b) and (8c)), Equations (14d) and (14e) are the discretized pharmacodynamics model for cancer cells (see (8d) and (8e)), and the constraint set (14f) is the linearized model for effective drug concentration (see (8f)).

The approximation quality and computational burden of Formulation (14) depends on the choice of discretization time step h and the method of bilinearity approximation, that is, McCormick relaxation or the discretization technique, as well as the choice of Δ in the latter method. We present the results of our computational experiments with respect to these factors in Section 5.

Finally, we note that the MILP framework can incorporate a wide range of objective functions. As mentioned earlier, the end-of-treatment tumor cell count is one of the modeling choices. Along this line, one may prioritize the count of certain cell types by including distinct coefficients for population variables in the current objective function. Another choice could be to minimize the cumulative tumor population over the treatment window or tumor population at a certain time other than the end of treatment, which can be easily modeled by linear functions.

3.2. Neoadjuvant Chemotherapy Under Uncertain Tumor Heterogeneity

In advanced stages of cancer, chemotherapy is often used as a form of neoadjuvant therapy to reduce a tumor to an operable size prior to tumor removal surgery (Senkus et al. 2015). In this section, we extend the proposed MILP model (14) to address the uncertainty of tumor heterogeneity in neoadjuvant chemotherapy planning. Under this uncertainty, the objective is to find a drug administration regimen that reduces the tumor to a clinically determined operable size with a high probability, which can be expressed by the following chance constraint:

$$\Pr\left\{\sum_{q\in\mathcal{Q}} N_{q,S} \le N_{\text{surg}}\right\} \ge 1 - \epsilon,\tag{15}$$

where N_{surg} denotes the clinically determined operable size for the tumor and ϵ is the probability of not meeting the target at the end of treatment period.

Let $\pi \in \mathbb{R}_+^{|\mathcal{Q}|}$ be a discrete random variable describing tumor heterogeneity, which can take on a value from the finite set $\{\pi^{(1)}, \ldots, \pi^{(K)}\}$, and denote the probability of a scenario $k \in \{1, \ldots, K\}$ by $\mu^{(k)} = \Pr\{\pi = \pi^{(k)}\}$. Given the logarithmic transformation of the cancer cell population variables in our model, we use the following more conservative constraints to enforce (15):

$$P_{q,S}^{(k)} \le P_{\text{surg}} + \ln\left(\frac{N_{q,0}^{(k)}}{\sum_{q \in \mathcal{Q}} N_{q,0}^{(k)}}\right) + P_{q,\infty}(1 - Z_{\text{surg}}^{(k)}), \ \forall \ q \in \mathcal{Q}, \ k \in \{1, \dots, K\},$$

$$(16a)$$

$$\sum_{k=1}^{K} \mu^{(k)} Z_{\text{surg}}^{(k)} \ge 1 - \epsilon, \tag{16b}$$

$$Z_{\text{surg}}^{(k)} \in \mathbb{B}, \ \forall k \in \{1, \dots, K\}, \tag{16c}$$

where $P_{\text{surg}} = \ln(N_{\text{surg}})$, $P_{q,\infty} = \ln(N_{q,\infty})$, and the superscript (k) denotes the value of previously defined variables under a realization scenario $k \in \{1, \dots, K\}$. The binary variable $Z_{\text{surg}}^{(k)}$ indicates whether the target is met under a scenario $k \in \{1, \dots, K\}$. The set of Constraints (16) is more conservative than the original Constraint (15) because every solution that satisfies (16) also satisfies (15), but the reverse does not necessarily hold. The implication of this relationship is that the optimal regimen of the chance-constrained model may actually satisfy the surgery requirement in more scenarios than those indicated by the optimal solution, hence leading to a success probability strictly better than $1 - \epsilon$. To establish the relation between (15) and (16), observe that, for a scenario k with $Z_{\text{surg}}^{(k)} = 1$,

$$\sum_{q \in \mathcal{Q}} N_{q,S}^{(k)} = \sum_{q \in \mathcal{Q}} e^{P_{q,S}^{(k)}} \leq \sum_{q \in \mathcal{Q}} e^{\ln \frac{\sum_{q \in \mathcal{Q}} N_{q,0}^{(k)}}{\sum_{q \in \mathcal{Q}} N_{q,0}^{(k)}}} = \sum_{q \in \mathcal{Q}} \left(\frac{N_{\text{surg}} N_{q,0}^{(k)}}{\sum_{q \in \mathcal{Q}} N_{q,0}^{(k)}} \right) = N_{\text{surg}} \frac{\sum_{q \in \mathcal{Q}} N_{q,0}^{(k)}}{\sum_{q \in \mathcal{Q}} N_{q,0}^{(k)}} = N_{\text{surg}},$$

where the inequality is because of (16a); $Z_{\text{surg}}^{(k)} = 0$ relaxes Constraint (16a) for a scenario k.

A conventional objective for such a chance-constrained optimization model is to maximize the probability of meeting the target, equivalently to minimize ϵ . A drawback of this objective is that, if the tumor size is not far from the clinical target, the model may achieve an objective value of $\epsilon = 0$ with a solution that may not lead to significant tumor shrinkage. Recall that the main clinical objective of chemotherapy is to reduce the cancer cell population as much as possible (American Cancer Society 2021c). In this regard, we also consider a shrinkage-based objective similar to our deterministic model. Note that, given a fixed value for ϵ , obtaining a success probability of $1 - \epsilon$ is guaranteed through the chance constraints (16a)–(16c) regardless of the objective function. Section 5 presents the results of our numerical study with both shrinkage- and probability-based objectives. Here, we present our stochastic model with an objective that minimizes the cancer cell population at the end of treatment under the most likely scenario. We assume $\mu^{(1)} \ge \mu^{(k)}$, $\forall k \in \{1, \ldots, K\}$; the neoadjuvant chance-

constrained MILP model is as follows:

$$\min \quad \sum_{q \in \mathcal{Q}} P_{q,S}^{(1)} \tag{17a}$$

s.t.
$$C_{d,s+1} = C_{d,s} - h \, \xi_d \, C_{d,s} + U_{d,s} / \mathcal{V}, \quad \forall d \in \mathcal{D}, s \in \{0, \dots, S-1\},$$
 (17b)

$$C_{d,0} = 0, \ \forall d \in \mathcal{D}, \tag{17c}$$

$$P_{q,s+1}^{(k)} = P_{q,s}^{(k)} + h\left(\Lambda\left(\ln(N_{q,\infty}^{(k)}) - P_{q,s}^{(k)}\right) - \sum_{d \in \mathcal{D}} \eta_{d,q} \exp(-\rho_{d,q} t(s)) E_{d,s}\right),$$

$$\forall q \in \mathcal{Q}, \ s \in \{0, \dots, S-1\}, \ k \in \{1, \dots, K\},$$
(17d)

$$P_{q,0}^{(k)} = \ln(N_{q,0}^{(k)}), \ \forall q \in \mathcal{Q}, \ k \in \{1, \dots, K\},\tag{17e}$$

$$(10a) - (10e), \ \forall \ d \in \mathcal{D}, \ s \in \{0, \dots, S\},$$
 (17f)

$$P_{q,S}^{(k)} \le P_{\text{surg}} + \ln\left(\frac{N_{q,0}^{(k)}}{\sum_{g \in \mathcal{Q}} N_{q,0}^{(k)}}\right) + P_{q,\infty}(1 - Z_{\text{surg}}^{(k)}), \ \forall q \in \mathcal{Q}, \ k \in \{1, \dots, K\},$$

$$(17g)$$

$$\sum_{k=1}^{K} \mu^{(k)} Z_{\text{surg}}^{(k)} \ge 1 - \epsilon, \tag{17h}$$

$$Z_{\text{surg}}^{(k)} \in \mathbb{B}, \ \forall k \in \{1, \dots, K\},\tag{17i}$$

$$(\mathbf{U}, \mathbf{C}, \mathbf{N}_{\text{neu}}, \mathbf{N}_{\text{lym}}) \in \hat{\mathcal{O}}. \tag{17j}$$

3.3. Analytical Results

Next, we present analytical results for the proposed combination chemotherapy optimization models. A main result is an error bound for the Euler's method approximation of the cell population state variables, which depend on the Euler's method approximation of the drug concentration state variables presented through Theorem 6 and Corollary 1. All proofs are provided in the e-companion; see Online Appendix B.

Theorems 1 and 2 show that, if drug administration is continuous, the state variables for drug concentration and cell population are uniquely defined by the control variables governing drug administration in the base formulation (8). Although administration of oral drugs is inherently discontinuous, they can be approximated arbitrarily well by continuous functions; hence, the uniqueness results hold for oral drugs as well.

Theorem 1. Suppose that, for a drug $d \in \mathcal{D}$, the administration function U_d is continuous in time. Then, the differential equation

$$\dot{C}_d(t) = -\xi_d C_d(t) + U_d(t)/\mathscr{V}, \ t \in [0, T],$$

governing the drug concentration function C_d , has a unique solution.

Theorem 2. Suppose that the administration functions for all drugs, that is, U_d , $\forall d \in \mathcal{D}$, are continuous in time. Then, for each cancer cell type $q \in \mathcal{Q}$, the differential equation

$$\dot{P}_{q}(t) = \Lambda(P_{q,\infty} - P_{q}(t)) - \sum_{d \in \mathcal{D}} \eta_{d,q} \exp(-\rho_{d,q} t) E_{d}(t), \ t \in [0, T],$$

governing the cell population function P_q , has a unique solution.

The next results concern the stability of Euler's method. A numerical method is absolutely stable for a region of time step discretization values if the global error can be bounded by the sum of truncation errors at each step. Absolutely stable numerical methods produce "reasonable results" for time-step values in the region of absolute stability (LeVeque 2007).

Theorem 3. Let $\{U_s\}_{s\in\mathbb{Z}_+}$ be a bounded sequence, and $\xi,h,\mathcal{V}>0$. Under the stability condition $h<\frac{2}{\xi}$, the difference equation

$$C_{s+1} = C_s - h \xi C_s + U_s / \mathcal{V}$$

is absolutely stable for all $s \in \mathbb{Z}_+$.

Theorem 4. Let $\{F_s\}_{s\in\mathbb{Z}_+}$ be a bounded sequence and $\Lambda,h>0$. Under the stability condition $h<\frac{2}{\Lambda'}$ the difference equation

$$P_{s+1} = P_s + h\left(\Lambda \left(P_{\infty} - P_s\right) - F_s\right),$$

is absolutely stable for all $s \in \mathbb{Z}_+$.

Concerning the stochastic model (17), the following result indicates that, if a feasible solution's effective concentration is dominated by another feasible solution's effective concentration, the second solution has a smaller end-of-treatment cancer cell population in all scenarios regardless of the objective function.

Theorem 5. Consider the stochastic model (17) with $\Delta h \leq 1$. Let $(\mathbf{E}^{[1]}, \mathbf{P}^{[1]})$ and $(\mathbf{E}^{[2]}, \mathbf{P}^{[2]})$ each be components of different feasible solutions. Suppose $E_{d,s}^{[1]} \geq E_{d,s}^{[2]}$ for all $d \in \mathcal{D}, s \in \{0,\ldots,S\}$. Then, $P_{q,S}^{[1],(k)} \leq P_{q,S}^{[2],(k)}$ for all $q \in \mathcal{Q}, k \in \{1,\ldots,K\}$.

Finally, Theorem 6 provides a global error bound for Euler's method applied to state variables that depend on another state variable estimated by Euler's method.

Theorem 6. Consider the system of differential equations

$$\dot{y}(t) = f(t, y, z), \ y(0) = y_0,$$

 $\dot{z}(t) = g(t, z), \ z(0) = z_0,$

and the Euler's approximation $\{(y_s, z_s)\}_{s=0}^S$ with step size h given by $y_{s+1} = y_s + hf(t(s), y_s, z_s)$ and $z_{s+1} = z_s + hg(t(s), z_s)$, where t(s) denotes the value of the continuous variable t at step s. Let $\lambda_z = \max\{|z_s - z_0|, s \in \{0, \dots, S\}\}$, and suppose g is continuous in both variables and Lipschitz continuous in its second variable, that is, there exists $L_g > 0$ such that, for all $t \in [0,T]$ and $u,v \in \mathbb{R}$ with $|u-z_0| \leq \lambda_z, |v-z_0| \leq \lambda_z$,

$$|g(t,u)-g(t,v)| \le L_g|u-v|.$$

Similarly, suppose f is continuous in all variables and Lipschitz continuous (with respect to the ℓ_1 norm) in its second and third variables with constant L_f . Furthermore, suppose y and z are twice continuously differentiable. Then, for all $s \in \{0, ..., S\}$,

$$|y_s - y(t(s))| \le \frac{h}{2} \frac{\alpha_z}{L_g} (e^{L_g T} - 1) + \frac{\alpha_y}{L_f} (e^{L_f T} - 1),$$

where $\alpha_z = \max_{\tau \in [0,T]} |\ddot{z}(\tau)|$ and $\alpha_y = \max_{\tau \in [0,T]} |\ddot{y}(\tau)|$.

Corollary 1. Let C(t) and $P_q(t)$, $\forall q \in \mathcal{Q}$ be the state variable functions for drug concentration and cell population, respectively, in an optimal solution to the (single-drug) chemotherapy optimization problem (8) without the effective concentration and operational constraints. Furthermore, suppose that C and P_q , $\forall q \in \mathcal{Q}$ are twice continuously differentiable, and let \widetilde{C} and \widetilde{P}_q , $\forall q \in \mathcal{Q}$ be the corresponding Euler's approximations with time-step h. Then,

$$\left| \sum_{q \in \mathcal{Q}} \tilde{P}_{q,S} - \sum_{q \in \mathcal{Q}} P_q(T) \right| \leq \sum_{q \in \mathcal{Q}} \frac{h}{2} \left| \frac{\alpha_C}{|\xi|} (e^{|\xi|T} - 1) + \frac{\alpha_q}{\max\{|\eta_q|, |\Lambda|\}} \right) (e^{\max\{|\eta_q|, |\Lambda|\}T} - 1),$$

where $\alpha_C = \max_{\tau \in [0,T]} |\ddot{C}(\tau)|$ and $\alpha_q = \max_{\tau \in [0,T]} |\ddot{P}_q(\tau)|$, $\forall q \in Q$.

4. Model Calibration

Though the proposed framework applies to many forms of cancer, we specify our numerical study for breast cancer, which kills more than 40,000 American women annually (American Cancer Society 2021a). We include three breast cancer drugs in our study: capecitabine, docetaxel, and etoposide; they are labeled 1, 2, and 3, respectively. To account for heterogeneity in the cell population, we include four tumor cell types: $0 \equiv$ "no resistance, all drugs", $1 \equiv$ "resistance, capecitabine only", $2 \equiv$ "resistance, docetaxel only", and $3 \equiv$ "resistance, etoposide only". We do not consider the case in which a cell type is resistant to multiple drugs because the drugs we consider have different mechanisms to attack tumor cells (Luqmani 2005).

The initial tumor size can vary substantially, depending on the progression of the disease, at the start of a treatment. Norton (1988) estimates the initial population size of untreated breast cancer patients as $N_0 = 4.8 \cdot 10^9$ cells. This estimate is supported by the fact that tumor detection usually does not occur before the tumor has 10^9 cells, 30 generations after the first malignant cell (Asachenkov et al. 1994, Cameron 1997). We use $2^{30} \approx 10^9$ cells as the initial cancer cell population. We estimate tumor heterogeneity, that is, $N_{q,0}$, $\forall q \in \{0,1,2,3\}$, through a branching process (e.g., Kimmel and Axelrod 2015). By simulating this process, we generate multiple scenarios concerning tumor heterogeneity and estimate the probability of realization for each scenario. The description of the

branching process and estimation of the initial cancer cell populations are provided in the e-companion; see Online Appendix C. We use these scenarios directly in our numerical study with the chance-constrained model (17); for the deterministic model (14), we use the (empirical) mean cell count for each tumor cell type in these scenarios. We note that it may take many years for a tumor to reach a detectable size, during which random cell mutations—captured by the branching process—play a substantial role in determining tumor composition. However, such an effect is negligible during the relatively short period of chemotherapy, and a Gompertzian model provides a reasonably accurate representation of tumor evolution for chemotherapy optimization. Norton (1988) estimates the steady-state tumor size as $N_{\infty} = 3.1 \cdot 10^{12}$ cells, which is supported by the maximum tumor size detected in mammograms (Cameron 1997); we set this asymptotic limit at approximately 10¹² cells in our models and assume that the steady-state ratio of a cell type population to the collective cell population remains close its ratio at the time of diagnosis. Following Harrold and Parker (2009), we estimate the Gompertz shape parameter by $\Lambda = \frac{1}{\tau} ln \left(\frac{ln(N_{\infty}/N_0)}{ln(N_{\infty}/2N_0)} \right)$, where τ is the doubling time of the tumor, set equal to five months in their work. For the white blood cell population dynamics, we follow Iliadis and Barbolosi (2000) and use $N_{w,0} = 8 \cdot 10^9$ cells per liter as the initial population and $v_w = 1.2 \cdot 10^9$ cells per liter per day and $v_w = 0.15$ per day as the production and turnover rates, respectively. Online Table D.1 summarizes the parameters used for population dynamics in our numerical study; see Online Appendix D.

We use the values reported in the literature for pharmacokinetics parameters, that is, elimination rate ξ_d , $\forall d \in \mathcal{D}$, effect compartment \mathscr{V} , and effectiveness threshold $\beta_{d,\text{eff}}$, $\forall d \in \mathcal{D}$ (Iliadis and Barbolosi 2000, Frances et al. 2011) and estimate the pharmacodynamics parameters based on published clinical data. In particular, we use the following administration regimens and the response rate observed in the corresponding clinical trial to estimate the effect of cytotoxic drugs on the cancer cell populations:

- Capecitabine (O'Shaughnessy et al. 2001): 1,255 mg/m² twice daily, six cycles of a two-week treatment period followed by a one-week rest period, response rate of 30%.
- Docetaxel (Chan et al. 1999): 100 mg/m², seven cycles of one-hour infusion every three weeks, response rate of 47%.
- Etoposide (Yuan et al. 2015): 60 mg/m² daily, 7 cycles of a 10-day treatment period followed by a 11-day rest period, response rate of 9%.

In clinical studies, the dose administration is commonly reported based on body surface area; we use 1.7 m² as an average person's body surface area in our study (Bonate 2011). The treatment (partial) response rate is defined as the percentage of the patients participating in a clinical trial who show 50% or more decrease in tumor size (diameter) as a result of the therapy (World Health Organization 1979). Details of pharmacodynamics parameters estimation are provided in the e-companion; see Online Appendix D. Given the narrow therapeutic margin of cytotoxic drugs, we make a conservative assumption that these drugs have the same fractional kill effect on the white blood cells as the cancer cells. Online Table D.2 displays the pharmacokinetics and pharmacodynamics parameters in our numerical study; see Online Appendix D.

We also use the simulation results of the aforementioned clinical trials to determine the operational constraints parameters concerning maximum drug concentration, maximum infusion rate, and maximum cumulative daily dose. This ensures that an (optimal) treatment solution stays within the common range of drug administration in practice. Capecitabine and etoposide are orally administered via pills of size 500 mg and 50 mg, respectively (Hande 1998, Sharma et al. 2006). Oral drugs are often taken with food, so we designate three time points within each day at which the oral drugs may be taken. Docetaxel use is constrained by a week-long rest period after each administration day. Finally, we use $\beta_{\text{neu}} = 2.5 \cdot 10^9$ and $\beta_{\text{lym}} = 1 \cdot 10^9$ cells per liter as the neutropenia and lymphocytopenia thresholds, respectively (Rosado et al. 2011, Mitrovic et al. 2012). Online Table D.3 in Online Appendix D summarizes the operational parameters used in our numerical study.

5. Computational Results

In this section, we present the results of our numerical study given the model specification and calibration details provided in Section 4. To solve the proposed mixed-integer linear programs, we used Gurobi 9.1.2 with default parameters on a machine with Intel(R) Core(TM) i7-3520M CPU @ 2.90 GHz and restricted the solution time for each instance to a maximum of two hours. Unless otherwise stated, we set the time step parameter h equal to one hour and use the constraint set (13) with $\Delta = \frac{1}{20}(N_{w,0} - \beta_w)$ to approximate the bilinear terms; to avoid explosion of the binary variables introduced in (13), we set the time step length of one day for the white blood cell count model. We present our results on the computational performance of the models under different discretization resolutions and bilinear approximation methods separately. Finally, we consider a treatment period of 21 days in

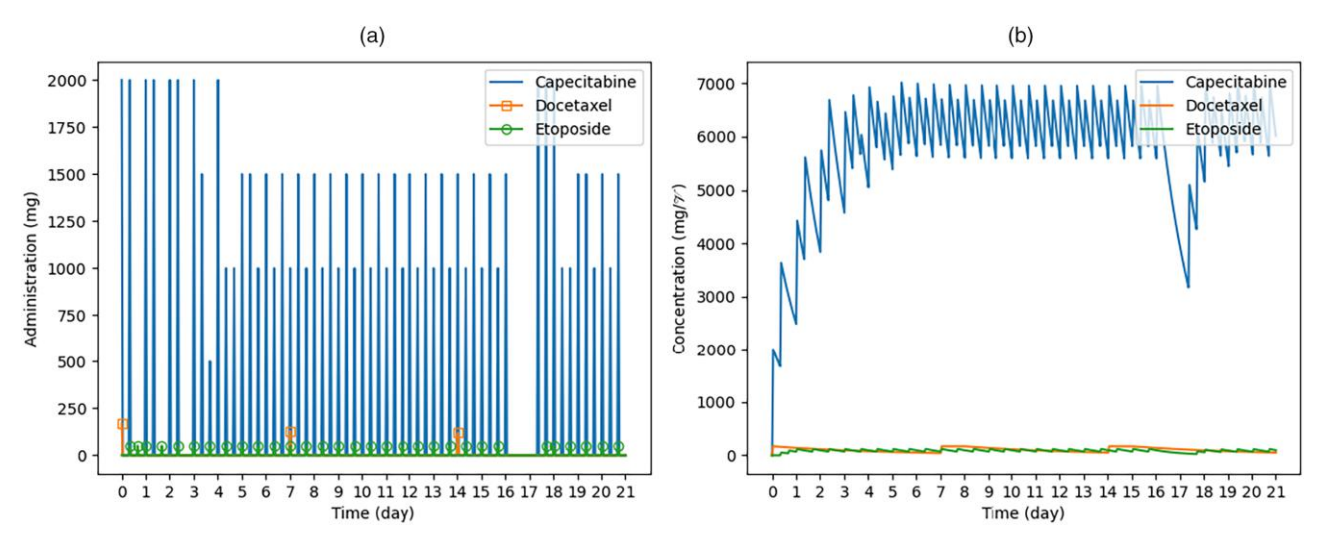
our numerical study, which is the common length for a chemotherapy cycle (Ershler 2006). Our computational results confirming the quality of Equation (6) in approximating Equation (5)—specifically, approximating the original Gompertz model of natural tumor growth by a linear ODE in our pharmacodynamics model—are provided in the e-companion; see Online Appendix E. The source code, data, and raw results of the experiments are available at Ajayi et al. (2023).

Figure 1 displays the optimal drug administration and concentration over the treatment period using the deterministic model (14). More details are provided in the e-companion; see Online Figure F.1 in Online Appendix F. From the optimal solution, the highest doses occur at the beginning of the treatment period for all drugs. For capecitabine and etoposide that can be administered frequently, the initial high doses make drug concentrations reach the maximum permissible levels, and after that, the administration regimens force relatively constant concentrations until an induced rest period on day 17; it is important to note that this rest period is not a modeling mandate. In fact, without an explicit rest constraint on the oral drug administration, the optimal solution shows a necessary rest period for these drugs to avoid the violation of toxicity (neutropenia) constraints, akin to mandated policies in clinical practice. Docetaxel, the intravenous drug, is administered weekly starting on the first day, because of the mandated rest period constraints.

The treatment effects on the cancer and white blood cell populations are illustrated in Figure 2. In this figure, $N \equiv$ nonresistant, $C \equiv$ capecitabine-resistant, $D \equiv$ docetaxel-resistant, and $E \equiv$ etoposide-resistant. All cancer cell types decrease fairly consistently (with respect to the logarithm) over time. The capecitabine- and etoposide-resistant cell types have similar outcomes; the docetaxel-resistant cell type shows a lower level of response to the treatment. Patently, the steepest descent belongs to the nonresistant cancer cell type. Regarding the white blood cell population, the neutropenia constraint is tight at the optimal solution, which is consistent with the clinical observation that neutropenia is often a toxicity of concern in chemotherapy (Pizzo 1993, Kosaka et al. 2015, Kasi and Grothey 2018).

An optimal regimen for a certain combination of drugs, that is, an optimal solution to MILP (14), depends on tumor properties, drug characteristics, and operational constraints. However, based on our case-study results, we conjecture that the current uniform standard-of-care regimens are not optimal in most cases. In the optimal regimen of our case study, all three drugs have higher administration doses in the early days than the rest of the treatment period, which aims at reaching the maximum permissible (effective) concentration as soon as possible. After that, drug administration tries to keep the concentration as close as possible to this level without violating the operational constraints. This pattern is well-justified to obtain the minimum tumor size at the end of the treatment because the kill effect of the drugs is highly determined by their concentrations; see Equation (14d). This pattern is also observed for capecitabine and etoposide (oral drugs) after the induced rest period on day 17; see Figure 1 and Online Figure F.1. This implies that having a rest period and then administrating a high dose (to make up for the consequent concentration drop) leads to a better objective value than keeping a continuous regular dose. We note that the feasibility of this pattern depends on the drugs' characteristics as well as the





Notes. (a) Administration. (b) Concentration.

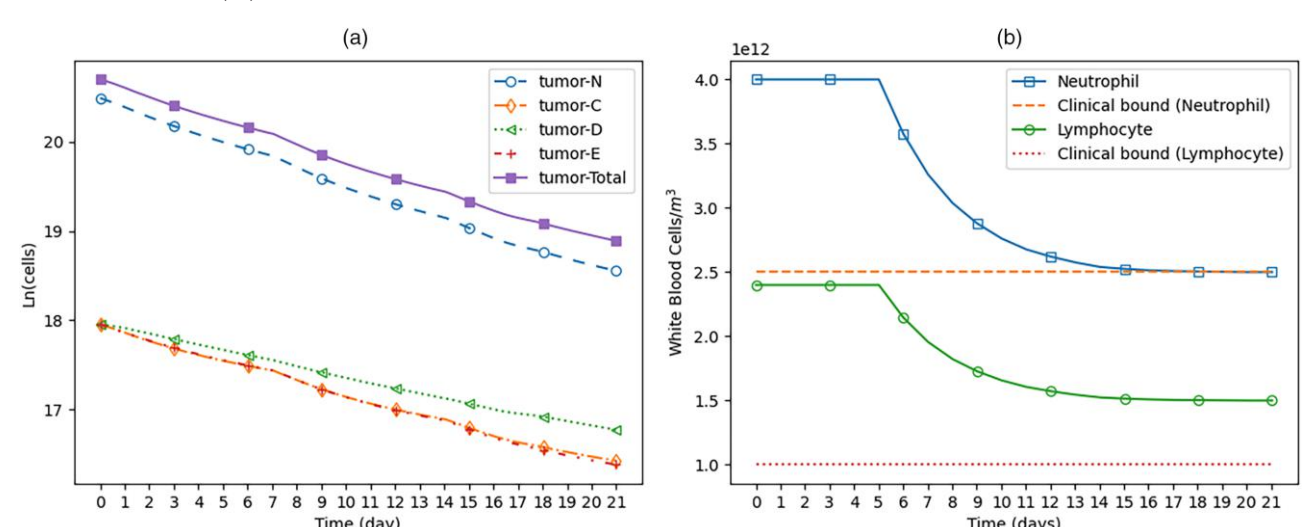


Figure 2. (Color online) Effect of the Optimal Drug Administration on Tumor and White Blood Cell Populations Given by the Deterministic Model (14)

Notes. (a) Cancer cell population (logarithmic scale). (b) White blood cell population.

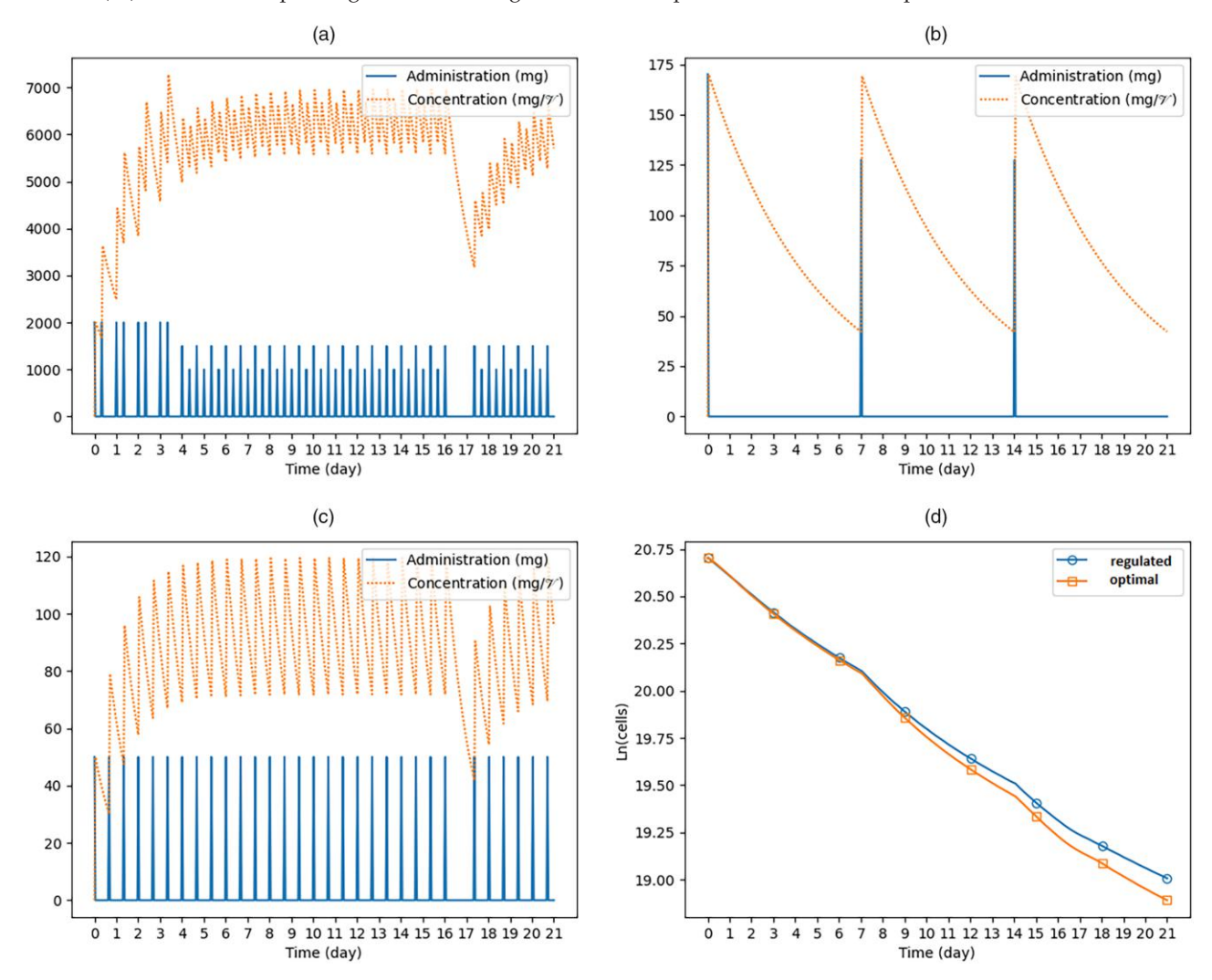
operational constraints. This can be observed by comparing the optimal regimens for capecitabine and etoposide in our case study. The maximum permissible daily doses for capecitabine and etoposide are equivalent to eight and two pills, respectively. Hence, the administration of capecitabine is more flexible than etoposide, and consequently, its optimal administration pattern is more distinguishable from a uniform pattern. This observation motivates conducting clinical trials with nonuniform regimens; any changes to standard of care must be evaluated and confirmed by clinical trials.

Standard regimens, including duration and frequency of rest periods, vary across individual chemotherapy drugs. For example, the drugs we consider in our case study analysis have the following individual rest periods with no standardized guidelines for their combination: (1) capecitabine: one-week rest period after two weeks of daily administration (O'Shaughnessy et al. 2001), (2) docetaxel: three-week rest period after a one-hour infusion (Chan et al. 1999), and (3) etoposide: 11-day rest period after 10 days of (daily) administration (Yuan et al. 2015). The ability of the proposed model to identify the necessity and optimality of a rest period to avoid toxicity (similar to clinical practice) paves the way to investigate optimal configuration of rest periods in combination chemotherapy and establishing standardized rest-period guidelines for an entire combination chemotherapy treatment period.

Regularity of drug administration is a logistic consideration for oral drugs as they are usually taken without direct medical supervision (Urquhart and De Klerk 1998). In this regard, we have considered converting the optimal solution presented in Figure 1 to a regulated administration plan. Figure 3 shows the result along with the corresponding tumor-shrinkage outcome; the difference in the cancer cell population between the optimal and regulated plans translates to less than 1 mm change in the tumor diameter. Note that, in construction of the regulated administration, we keep the induced rest period on day 17 because ignoring this period leads to a violation of the neutropenia constraint. We acknowledge that regularity of the administration regimen for oral drugs can be enforced by additional constraints; however, such patterns must be devised carefully as they can be too restrictive on the outcome. Finally, we point out that, given the pill sizes and maximum dose and concentration constraints for the oral drugs that we consider, the difference between the optimal and regulated plans mainly concerns the administration of capecitabine, which is weaker than etoposide based on the fractional kill effect parameter values.

In the next phase of our experiments, we investigated the impact of different discretization resolutions on the computational performance of (14) by varying the time step parameter h from four hours (240 minutes) to 15 minutes. Table 1 summarizes the results. The (optimality) gaps are solver-generated and concern the difference between the mixed-integer solutions and their linear program–relaxation bounds at the time of algorithm termination; the gap of 0.01% is the solver's default value within which it considers an incumbent solution optimal. Given the initial objective value of $\sum_{q=0}^{3} P_{q,0} = 74.34$ at the start of the treatment, there is little evidence that

Figure 3. (Color online) Regulated Drugs Administration (and Concentration) Based on the Optimal Solution of the Deterministic Model (14) and the Corresponding Tumor-Shrinkage Outcome Compared with That of the Optimal Solution



Notes. (a) Capecitabine administration and concentration. (b) Docetaxel administration and concentration. (c) Etoposide administration and concentration. (d) Cancer cell population (logarithmic scale).

the discretization resolution (within the tested range) substantially impacts the optimal objective value, in accordance with our stability results; all tested time step values satisfy the stability conditions of Theorems 3 and 4. However, it does impact the model's solvability because, as h decreases, the number of variables and constraints increase. The gap for the model with h = 15 minutes was 0.09%, the highest among the tested values.

We also examine the impact of different approximation methods for bilinear terms, that is, Constraints (12) and (13); for the latter, we considered two different discretization intervals for the white blood cell count, that is, $\Delta = \frac{1}{20}(N_{w,0} - \beta_w)$ and $\Delta = \frac{1}{40}(N_{w,0} - \beta_w)$. Recall that $N_{w,0}$ and β_w denote upper and lower bounds on the white blood cell count, respectively. The results are presented in Table 2, in which "Continuous" refers to the McCormick relaxation method, that is, the constraint set (12), and "Discrete" to the (modified) method of Gupte et al. (2013), that is, the constraint set (13). As expected, the McCormick relaxation method leads to a lower optimal objective value because of its flexibility. This method, however, does not provide a means to control the approximation quality of the bilinear terms. The solvability of the model decreases as more integer variables are introduced through refining the discretization interval in the method of Gupte et al. (2013).

Next, we present the results of our numerical study with the chance-constrained optimization model (17). We simulated a branching process to generate a set of scenarios describing the heterogeneity of the tumor. Details of the branching process and scenario generation are provided in Online Appendix C. Table 3 displays the (logarithm of) cancer cell populations and realization probability for each scenario. Based on the branching process,

h, min	Objective value	Run time, s	Cons	Vars	IVars	BVars	Gap, %
240	68.09	1,163	8,547	3,759	714	588	< 0.01
120	68.12	7,200	11,571	5,523	840	714	0.02
60	68.13	2,029	17,619	9,051	1,092	966	< 0.01
30	68.21	7,200	29,715	16,107	1,596	1,470	0.02
15	68.24	7,200	53,907	30,219	2,604	2,478	0.09

Table 1. Solver Statistics for Different Time Step Values (h)

there is a single dominant scenario (scenario 1) with the associated probability of more than 0.77 in which the nonresistant cell type has the largest cell count. The probability of a scenario in which a drug-resistant cell type has the largest cell count is less than 0.02. Although the size of the drug-resistant part of a tumor is expected to be smaller than the nonresistant part, it can become dominant without treatment.

The initial cancer cell population in all scenarios is 10^9 cells, which translates to a tumor with a diameter of about 25 mm (Del Monte 2009). Whereas the operable size of a tumor must be determined clinically based on the tumor location and patient's health conditions, the diameter of 20 mm is commonly considered the border of stage II and stage III breast cancer (Senkus et al. 2015). Thus, in our study, we assume $N_{\rm surg} = 0.4 \bullet 10^9$ cells, which translates to a diameter of less than 20 mm. We also set $\epsilon = 0.05$, indicating that the desired probability of reaching an operable tumor size at the end of treatment period is at least 0.95. Using the discrete approximation of the bilinear terms with $\Delta = \frac{1}{20}(N_{w,0} - \beta_w)$ and setting the time step h equal to one hour, the neoadjuvant chance-constrained optimization model (17) contained 27,205 variables (1,102 integer, 976 binary) and 35,804 constraints; the solver found an optimal solution in about 17 minutes with the optimal objective value of 67.99. Figure 4 illustrates the treatment effect on cancer cell populations under scenarios 1–4; these are the scenarios with the realization probability of at least 0.05. More details on the output of the chanced-constrained model (17) as well as its counterpart with a probability-based objective, that is, minimize ϵ subject to (17b)–(17j), are provided in the e-companion; see Online Appendix F. As stated earlier and illustrated in Online Figures F.4 and F.5, the probability-based objective leads to inferior tumor shrinkage compared with Formulation (17).

5.1. Sensitivity Analysis

The proposed optimization models involve several parameters that need to be estimated based on clinical data and a patient's biological characteristics. In this section, we present the results of our analysis to determine the sensitivity of an optimal solution and objective value of the combination chemotherapy optimization problem (14) to these parameters.

Figure 5 illustrates the results of the sensitivity analysis with respect to the pharmacokinetics and pharmacodynamics parameters. We use clinical data to estimate the fractional kill effect parameter of each drug for the nonresistant cell type, that is, $\eta_{d,0}$, and set $\eta_{d,q} = 0.25 \, \eta_{d,0}$, $\forall \, q \in \{1,2,3\}$, to account for drug-resistance in our numerical study; see Online Appendix D for more information. We also assume that temporal resistance is constant across the cancer cell types, that is, $\rho_{d,q} = \rho_{d,0}$, $\forall \, q \in \{1,2,3\}$. Thus, for these parameters, we focus on $\eta_{d,0}$ and $\rho_{d,0}$. For each drug, we varied the corresponding parameters in 10% increments as the other parameters of the model remained constant and measured the corresponding impact on the optimal objective value. To provide a convenient comparison, in Figure 5, the horizontal axes demonstrate (changed) parameter values as a fraction of the original value; the vertical axes display the optimal objective value, that is, $\sum_{a \in \mathcal{O}} P_{a,S}^*$.

In general, the optimal objective value of the combination chemotherapy optimization problem (14) is more sensitive to the fractional kill effect of a drug on cancer cells than any other pharmacokinetics or pharmacodynamics parameter. Based on Figure 5(b), docetaxel, the intravenous drug, is the most influential on the optimal objective value among the considered drugs; the oral drugs, capecitabine and etoposide, are less impactful and show very similar patterns. Apart from the fractional kill effect on cancer cells, the objective is most sensitive to the drug elimination rate. Recall that, for a drug d, the elimination rate ξ_d determines how fast the drug concentration in the body declines. Figure 5(a) suggests docetaxel has the most influential elimination rate on the

Table 2. Solver Statistics for Different Bilinearity Approximation Methods

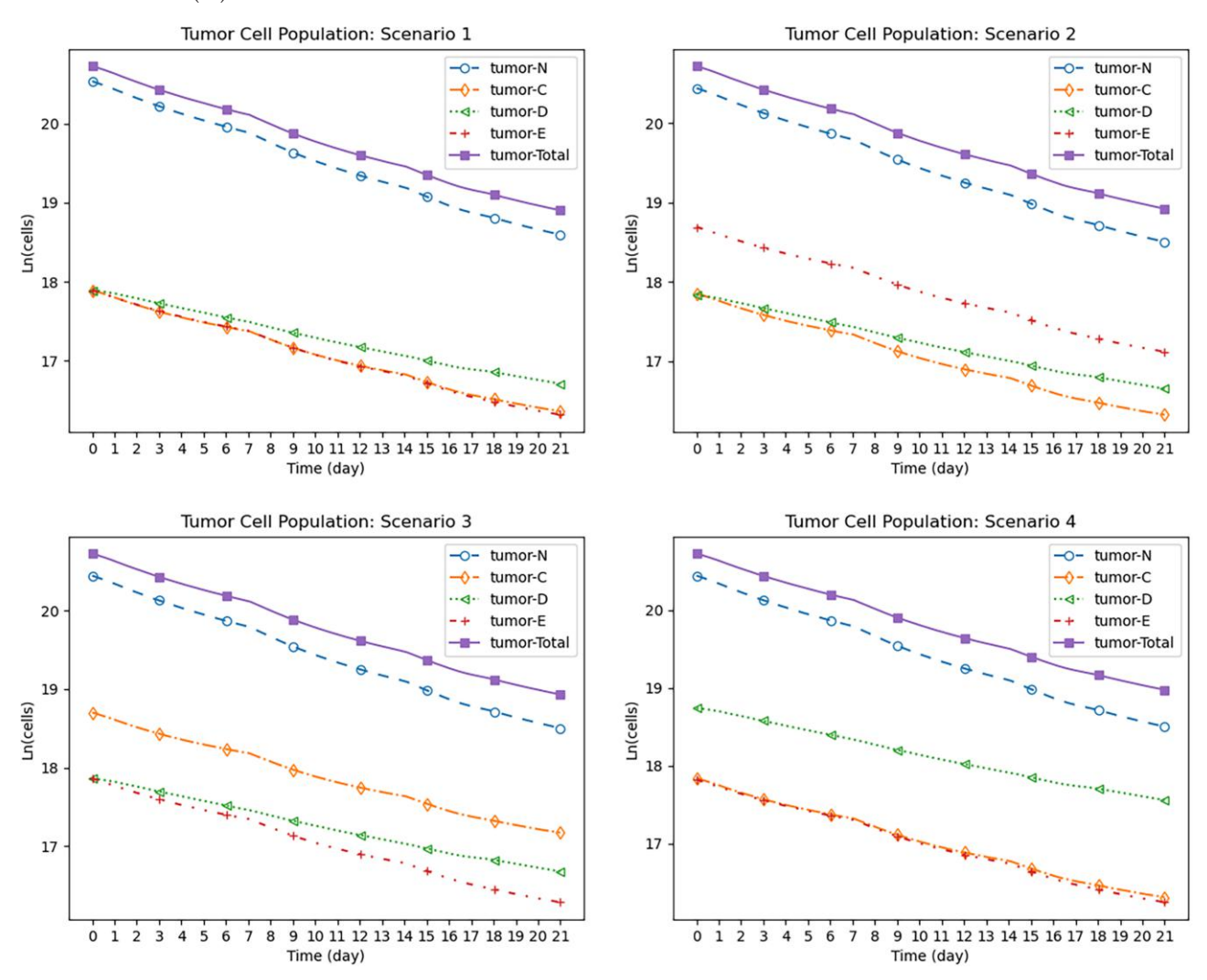
Method	Δ	Objective value	Run-time, s	Cons	Vars	IVars	BVars	Gap, %
Continuous	-	68.01	387	12,579	7,350	651	525	<0.01
Discrete	1/20	68.13	2,029	17,619	9,051	1,092	966	<0.01
Discrete	1/40	68.14	7,200	22,659	10,731	1,512	1,386	0.13

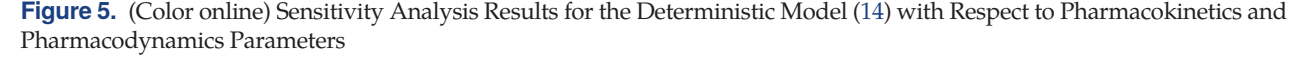
Table 3. Simulated Scenarios Generated by a Branching Process

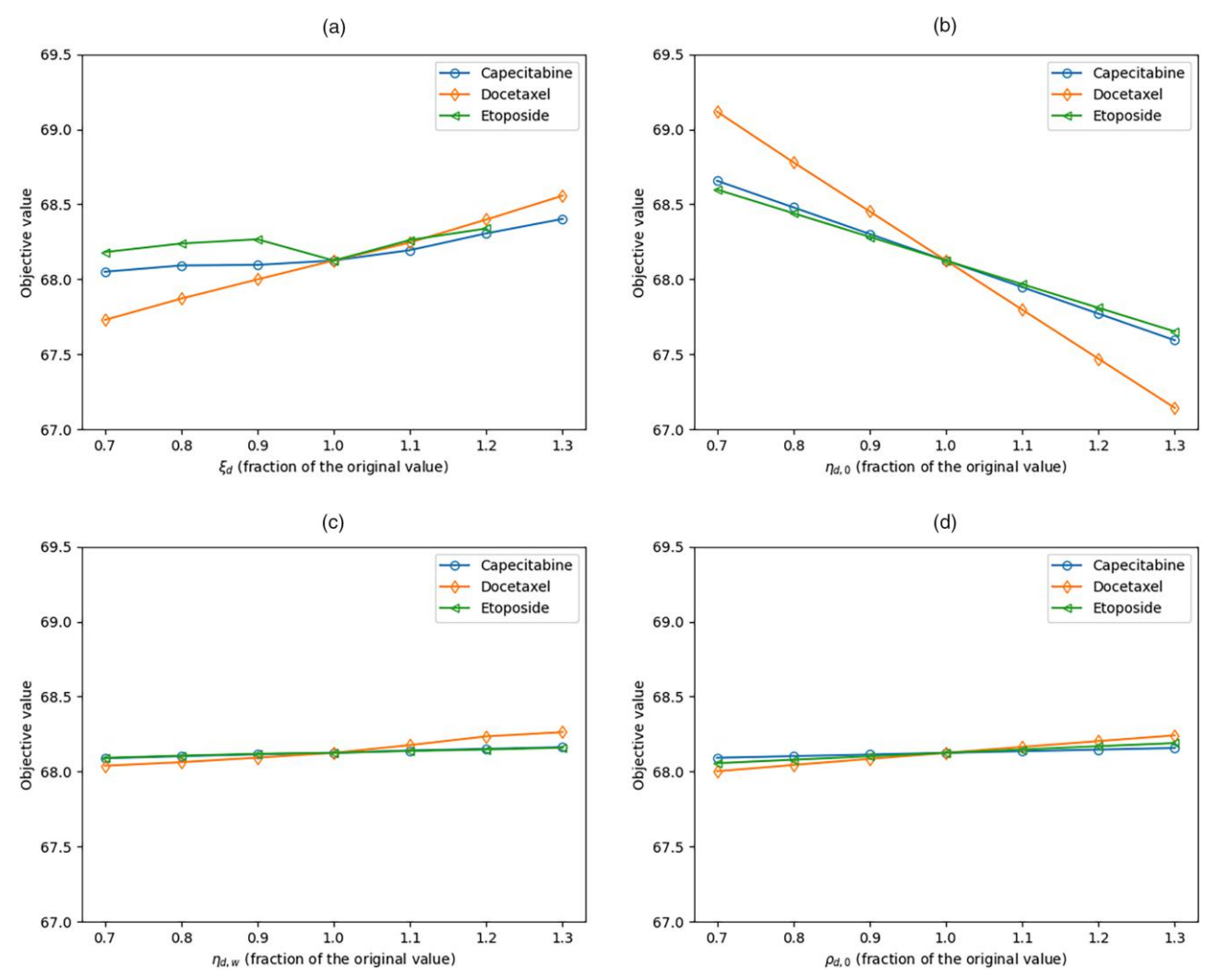
Scenario	Nonresist. (0)	Capecresist. (1)	Docetresist. (2)	Etoporesist. (3)	Prob.
1	20.53	17.89	17.89	17.89	0.7705
2	20.44	17.85	17.83	18.69	0.0619
3	20.44	18.70	17.86	17.86	0.0603
4	20.44	17.84	18.74	17.82	0.0579
5	20.22	19.50	17.74	17.72	0.0109
6	20.23	17.71	19.49	17.71	0.0109
7	20.25	17.72	17.67	19.46	0.0103
8	19.80	17.35	17.45	20.09	0.0064
9	19.81	17.20	20.10	17.28	0.0059
10	19.80	20.11	17.18	17.39	0.0050

objective value as well. It is important to note that docetaxel has a mandated one-week rest period; hence, the model has very little flexibility for administration of this drug. In other words, as opposed to oral drugs that can be administrated frequently to keep their concentrations constantly high during the treatment period, the docetaxel concentration is much lower than its maximum level for most of the treatment period. Because of this operational constraint, changes to the elimination rate of this drug directly influence its concentration profile and lead to relatively high impacts on the optimal objective value. As shown in Figure 5, (c) and (d), the model shows

Figure 4. (Color online) Treatment Effect on Tumor Cell Populations Under Scenarios 1–4 Given by the Neoadjuvant Chance-Constrained Model (17)







Notes. (a) Elimination rate. (b) Kill effect on cancer cells. (c) Kill effect on white blood cells. (d) Temporal resistance.

much less sensitivity to the parameters representing fractional kill effect on white blood cells and temporal resistance, that is, $\eta_{d,w}$ and $\rho_{d,0}$. The low impact of $\eta_{d,w}$ comparative to $\eta_{d,0}$ is justified by the fact that the model has a tumor shrinkage–based objective.

Another important observation regarding the impact of operational constraints on the optimal objective value of Model (14) concerns the elimination rate of etoposide; see Figure 5(a). The increasing patterns observed from 0.7 to 0.9 (as fractions of the original value) and from 1.0 to 1.2 are justified by the fact that higher elimination rates lead to lower drug concentrations and smaller effects on tumor cells. However, a better objective value is obtained when the elimination rate changes from 0.9 to 1.0. This is because the optimal administration regimen for etoposide changes in this interval. In fact, a higher elimination rate allows the model to administer etoposide more frequently without violation of the maximum permissible concentration given the discrete administration times. A similar phenomenon underlies the change of slope observed in this figure for capecitabine. Finally, we note that the value of the elimination rate parameter of a drug is physically restricted to $\xi = 1.0 \text{ day}^{-1}$; hence, the etoposide curve in Figure 5(a) terminates at $\xi = 1.2 \times 0.8 = 0.96 \text{ day}^{-1}$.

Aside from the pharmacokinetics and pharmacodynamics parameters, we evaluated the impact of changes to operational parameters governing the combination chemotherapy optimization model (14). In particular, we investigated changes to the maximum permissible dose (and concentration) for each drug and the neutropenia threshold. Recall that the maximum permissible doses (and concentrations) used in our numerical study are

69.5 69.5 Capecitabine Docetaxel Etoposide 69.0 Objective value Objective value 68.5 68.5 68.0 67.5 67.5 67.0 0.75 1.00 0.7 0.8 0.9 1.0 1.1 1.2 1.3 1.25 Maximum permissible daily dose (fraction of the original value) β_{neu} (fraction of the original value)

Figure 6. (Color online) Sensitivity Analysis Results for the Deterministic Model (14) with Respect to Operational Parameters

Notes. (a) Maximum permissible dose (and concentration). (b) Neutropenia threshold.

based on common administration regimens in clinical trials. For capecitabine, the clinical administration dose translates to eight pills per day, restricted to at most four pills per meal; we denote this regimen by 8/4 hereafter. We considered increasing these limits to 10/5 and decreasing them to 6/3. Based on the new values, we calculated the maximum permissible doses and drug concentration through simulation of the corresponding clinical trial. Similarly, for etoposide, we considered changing the current administration regimen of 2/1 to 3/2 and 1/1. In the presentation of the result to follow, with a slight abuse of the term "dose," we demonstrate these changes as 25% increase and decrease to the maximum permissible dose. For the intravenous drug, docetaxel, we directly applied the 25% increase and decrease to the current maximum permissible daily dose and infusion rate; similar to oral drugs, we obtain the corresponding maximum permissible concentration from simulation of the corresponding clinical trial with the new administration values. Figure 6(a) illustrates the results. According to this figure, the maximum permissible dose (and concentration) constraints are the most restrictive for etoposide, and their relative relaxation can significantly impact the treatment outcome. Note that the new optimal solutions satisfy the neutropenia constraint; under higher administration doses, the count of neutrophils never falls below the neutropenia threshold, but it reaches this level much earlier and stays there for the rest of the treatment period. Such an increased dose may lead to side effects other than neutropenia, which are not captured by our model.

Normal white blood cell counts vary across patients; different individuals may have different white blood cell thresholds for the associated side effects. In our sensitivity analysis, we changed the neutropenia threshold in 10% increments and measured its impact on the optimal objective value; the results are illustrated in Figure 6(b). Given the tightness of the neutropenia constraint, as mentioned before, deterioration of the optimal objective value because of the increase of neutropenia threshold is well-justified. This figure also shows that decreasing the neutropenia threshold below 90% of the current level will not affect the optimal objective value given the specified values for other parameters in our model. This observation demonstrates that, below this level, other operational constraints, that is, maximum permissible doses and concentrations, are the driving factors.

Sensitivity analysis with respect to the chance parameter ϵ in the stochastic model (17) is also of great interest. Such results, however, are highly dependent on tumor composition scenarios and their probabilities. For example, given three scenarios with the probabilities of 0.40, 0.35, and 0.25, the closest meaningful choice of ϵ to $\epsilon = 0$ would be $\epsilon = 0.25$. Therefore, such an effort must be equally focused on the branching process to generate rigorous and reliable results, which is beyond the scope of this paper. The choice of $\epsilon = 0.05$ in our numerical study follows the common engineering practice (95% confidence). For clinical applications, this threshold must be determined on a case-by-case basis, considering the patients' conditions and clinicians' judgment.

6. Conclusion

This paper presents a mixed-integer linear programming model for combination chemotherapy optimization, which seeks to find an optimal administration dose and schedule for cytotoxic drugs by minimizing the cancer cell population at the end of a treatment period. As opposed to previous works that often ignore operational

considerations or low white blood cell counts as a toxic effect, we incorporate these constraints. We also extend this model to account for the uncertainty of tumor heterogeneity and present a chanced-constrained model for neoadjuvant chemotherapy. We use the literature and published clinical data to calibrate our model parameters for a case of breast cancer and present the results of our numerical study. We perform sensitivity analyses to identify the most influential parameters on the model outcomes. Our models provide a framework for the exploration of new, individualized dose guidelines.

The computational framework proposed in this paper is not limited to chemotherapy and cytotoxic drugs; it can be extended to other drug-based treatments that necessitate making discrete decisions in continuously evolving environments. For example, our methodology may be applicable to designing colistin-based antibiotic treatment against Gram-negative bacteria, which can develop colistin resistance within its colony (Yang et al. 2017). However, it is important to note that biological systems are extremely complex, and every computational model representing these systems has its own limitations, which need to be considered for clinical applications. Whereas the proposed model carefully considers the representational validity of its pharmacokinetics and pharmacodynamics components as well as the operational constraints of chemotherapy, the quality of its outcomes highly relies on the accuracy of the model parameters; small errors in estimating these parameters may lead to significantly different clinical outcomes. In addition, our model only considers the effect of chemotherapy on the immune system and the count of white blood cells as the measure of treatment toxicity, whereas chemotherapy may come with several different side effects. For example, chemotherapy may highly increase the risk of acute kidney injury (Li et al. 2017); clinical applications must consider all major side effects of chemotherapy.

An immediate research direction to extend this work would be to investigate the optimal configuration of rest periods over an entire combination chemotherapy treatment period. Some other potential directions stemming from this work include improving estimates of model (pharmacokinetics and pharmacodynamics) parameters, considering other drugs or types of cancer in the numerical study, and factoring additional toxicities. We also encourage future researchers to extend this work by incorporating the risk of metastatic disease into the chemotherapy optimization problem. Another line of research could focus on multidrug resistance and its effect on the risk of treatment failure. Performing sensitivity analysis with respect to the chance parameter ϵ , with equal focus on the branching process, is another direction to extend this work.

Acknowledgments

The authors thank the three anonymous referees for their helpful suggestions and constructive comments. The authors also thank Jeffrey Myers and Cem Dede of the University of Texas MD Anderson Cancer Center; Adam Palmer of the University of North Carolina; and David Mildebrath, Soheil Hemmati, Saumya Sinha, Can Camur, and Shengchao Lin of Rice University for their helpful comments.

References

Abécassis J, Hamy A, Laurent C, Sadacca B, Bonsang-Kitzis H, Reyal F, Vert JP (2019) Assessing reliability of intratumor heterogeneity estimates from single sample whole exome sequencing data. *PLoS One* 14(11):e0224143.

Ajayi T, Hosseinian S, Schaefer AJ, Fuller CD (2023) Combination chemotherapy optimization with discrete dosing. https://dx.doi.org/10.1287/ijoc.2022.0207.cd, https://github.com/INFORMSJoC/2022.0207.

Al-Khayyal F, Falk J (1983) Jointly constrained biconvex programming. Math. Oper. Res. 8(2):273–286.

Alam M, Hossain M, Algoul S, Majumader MAA, Al-Mamun MA, Sexton G, Phillips R (2013) Multi-objective multi-drug scheduling schemes for cell cycle specific cancer treatment. *Comput. Chemical Engrg.* 58:14–32.

American Cancer Society (2021a) Cancer facts & figures 2021. Accessed November 2, 2021, https://www.cancer.org/research/cancer-facts-statistics/all-cancer-facts-figures-2021.html.

American Cancer Society (2021b) Cancer treatment & survivorship facts & figures 2019–2021. Accessed November 2, 2021, https://www.cancer.org/research/cancer-facts-statistics/survivor-facts-figures.html.

American Cancer Society (2021c) Chemotherapy. Accessed November 2, 2021, https://www.cancer.org/treatment/treatments-and-side-effects/treatment-types/chemotherapy.html.

Asachenkov A, Marchuk G, Mohler R, Zuev S (1994) Disease Dynamics, 1st ed. (Birkhäuser, Basel, Switzerland).

Baker S, Sparreboom A, Verweij J (2006) Clinical pharmacokinetics of docetaxel. Clinical Pharmacokinetics 45(3):235–252.

Bonate P (2011) Pharmacokinetic-Pharmacodynamic Modeling and Simulation, vol. 20 (Springer, New York).

Butcher J (2007) Runge-Kutta methods. Scholarpedia 2(9):3147.

Cajal S, Sesé M, Capdevila C, Aasen T, De Mattos-Arruda L, Diaz-Cano SJ, Hernández-Losa J, Castellví J (2020) Clinical implications of intratumor heterogeneity: Challenges and opportunities. *J. Molecular Medicine* 98(2):161–177.

Cameron D (1997) Mathematical modelling of the response of breast cancer to drug therapy. J. Theoretical Medicine 1(2):137–151.

Chan S, Friedrichs K, Noel D, Pintér T, Van Belle S, Vorobiof D, Duarte R, et al. (1999) Prospective randomized trial of docetaxel vs. doxorubicin in patients with metastatic breast cancer. *J. Clinical Oncology* 17(8):2341–2354.

Coldman A, Goldie J (1983) A model for the resistance of tumor cells to cancer chemotherapeutic agents. Math. Biosciences 65(2):291–307.

Coldman A, Murray J (2000) Optimal control for a stochastic model of cancer chemotherapy. Math. Biosciences 168(2):187-200.

Costa M, Boldrini J (1997) Chemotherapeutic treatments: A study of the interplay among drug resistance, toxicity and recuperation from side effects. *Bull. Math. Biol.* 59(2):205–232.

Day R (1986) Treatment sequencing, asymmetry, and uncertainty: Protocol strategies for combination chemotherapy. *Cancer Res.* 46(8):3876–3885.

de Pillis L, Gu W, Fister K, Head T, Maples K, Murugan A, Neal T, Yoshida K (2007) Chemotherapy for tumors: An analysis of the dynamics and a study of quadratic and linear optimal controls. *Math. Biosciences* 209(1):292–315.

Del Monte U (2009) Does the cell number 109 still really fit one gram of tumor tissue? Cell Cycle 8(3):505–506.

d'Onofrio A, Ledzewicz U, Maurer H, Schättler H (2009) On optimal delivery of combination therapy for tumors. *Math. Biosciences* 222(1):13–26.

Ebata T, Hirano S, Konishi M, Uesaka K, Tsuchiya Y, Ohtsuka M, Kaneoka Y, et al. (2018) Randomized clinical trial of adjuvant gemcitabine chemotherapy vs. observation in resected bile duct cancer. *J. British Surgery* 105(3):192–202.

Ershler WB (2006) Capecitabine monotherapy: Safe and effective treatment for metastatic breast cancer. Oncologist 11(4):325–335.

Floares A, Floares C, Cucu M, Lazar L (2003) Adaptive neural networks control of drug dosage regimens in cancer chemotherapy. *Proc. Internat. Joint Conf. Neural Networks*, vol. 1 (IEEE, Piscataway, NJ), 154–159.

Frances N, Claret L, Bruno R, Iliadis A (2011) Tumor growth modeling from clinical trials reveals synergistic anticancer effect of the capecitabine and docetaxel combination in metastatic breast cancer. *Cancer Chemotherapy Pharmacology* 68(6):1413–1419.

Gerlinger M, Rowan A, Horswell S, Larkin J, Endesfelder D, Gronroos E, Martinez P, et al. (2012) Intratumor heterogeneity and branched evolution revealed by multiregion sequencing. *New England J. Medicine* 366(10):883–892.

Gupte A, Ahmed S, Cheon M, Dey S (2013) Solving mixed integer bilinear problems using MILP formulations. SIAM J. Optim. 23(2):721–744. Hande K (1998) Etoposide: Four decades of development of a topoisomerase II inhibitor. Eur. J. Cancer 34(10):1514–1521.

Harrold J, Parker R (2009) Clinically relevant cancer chemotherapy dose scheduling via mixed-integer optimization. *Comput. Chemical Engrg.* 33(12):2042–2054.

He Q, Zhu J, Dingli D, Foo J, Leder KZ (2016) Optimized treatment schedules for chronic myeloid leukemia. PLOS Comput. Biol. 12(10):e1005129.

Hu Q, Sun W, Wang C, Gu Z (2016) Recent advances of cocktail chemotherapy by combination drug delivery systems. *Adv. Drug Delivery Rev.* 98:19–34.

Hu Z, Sun R, Curtis C (2017) A population genetics perspective on the determinants of intratumor heterogeneity. Biochimica Biophysica Acta (BBA)-Rev. Cancer 1867(2):109–126.

Iliadis A, Barbolosi D (2000) Optimizing drug regimens in cancer chemotherapy by an efficacy-toxicity mathematical model. *Comput. Biomedical Res.* 33(3):211–226.

Itik M, Salamci M, Banks S (2009) Optimal control of drug therapy in cancer treatment. Nonlinear Anal. Theory *Methods Appl.* 71(12):e1473–e1486. Jacqmin P, Snoeck E, Van Schaick E, Gieschke R, Pillai P, Steimer JL, Girard P (2007) Modelling response time profiles in the absence of drug concentrations: Definition and performance evaluation of the K–PD model. *J. Pharmacokinetics Pharmacodynamics* 34(1):57–85.

Kasi P, Grothey A (2018) Chemotherapy-induced neutropenia as a prognostic and predictive marker of outcomes in solid-tumor patients. Drugs 78(7):737–745.

Kimmel M, Axelrod D (2015) Branching Processes in Biology, 2nd ed. (Springer, New York).

Kosaka Y, Rai Y, Masuda N, Takano T, Saeki T, Nakamura S, Shimazaki R, Ito Y, Tokuda Y, Tamura K (2015) Phase III placebo-controlled, double-blind, randomized trial of pegfilgrastim to reduce the risk of febrile neutropenia in breast cancer patients receiving docetaxel/dyclophosphamide chemotherapy. *Supportive Care Cancer* 23(4):1137–1145.

Laird A, Tyler SA, Barton A (1965) Dynamics of normal growth. *Growth* 29(3):233–248.

LeVeque R (2007) Finite Difference Methods for Ordinary and Partial Differential Equations (Society for Industrial and Applied Mathematics, Philadelphia).

Li S, Liu J, Virnig B, Collins A (2017) Association between adjuvant chemotherapy and risk of acute kidney injury in elderly women diagnosed with early-stage breast cancer. *Breast Cancer Res. Treatment* 161(3):515–524.

Liang Y, Leung K, Mok T (2006) A novel evolutionary drug scheduling model in cancer chemotherapy. *IEEE Trans. Inform. Tech. Biomedicine* 10(2):237–245.

Luqmani Y (2005) Mechanisms of drug resistance in cancer chemotherapy. Medical Principles Practice 14(suppl. 1):35-48.

Mariotti V, Han H, Ismail-Khan R, Tang SC, Dillon P, Montero AJ, Poklepovic A, et al. (2021) Effect of taxane chemotherapy with or without indoximod in metastatic breast cancer: A randomized clinical trial. *JAMA Oncology* 7(1):61–69.

Martin R (1992) Optimal control drug scheduling of cancer chemotherapy. Automatica J. IFAC 28(6):1113-1123.

Martin R, Fisher M, Minchin R, Teo K (1990) A mathematical model of cancer chemotherapy with an optimal selection of parameters. *Math. Biosciences* 99(2):205–230.

Martin R, Fisher M, Minchin R, Teo K (1992a) Low-intensity combination chemotherapy maximizes host survival time for tumors containing drug-resistant cells. *Math. Biosciences* 110(2):221–252.

Martin R, Fisher M, Minchin R, Teo K (1992b) Optimal control of tumor size used to maximize survival time when cells are resistant to chemotherapy. *Math. Biosciences* 110(2):201–219.

McCormick G (1976) Computability of global solutions to factorable nonconvex programs: Part I—Convex underestimating problems. *Math. Programming* 10(1):147–175.

Mitrovic Z, Perry A, Suzumiya J, Armitage JO, Au WY, Coiffier B, Holte H, et al. (2012) The prognostic significance of lymphopenia in peripheral T-cell and natural killer/T-cell lymphomas: A study of 826 cases from the International Peripheral T-cell Lymphoma Project. *Amer. J. Hematology* 87(8):790–794.

Murray J (1990) Some optimal control problems in cancer chemotherapy with a toxicity limit. Math. Biosciences 100(1):49-67.

Murray J (1994) Optimal drug regimens in cancer chemotherapy for single drugs that block progression through the cell cycle. *Math. Biosciences* 123(2):183–213.

Murray J (1997) The optimal scheduling of two drugs with simple resistance for a problem in cancer chemotherapy. *Math. Medicine Biol.* 14(4):283–303.

Nanda S, Moore H, Lenhart S (2007) Optimal control of treatment in a mathematical model of chronic myelogenous leukemia. *Math. Biosciences* 210(1):143–156.

Nøhr-Nielsen A, Bagger SO, Brünner N, Stenvang J, Lund TM (2020) Pharmacodynamic modelling reveals synergistic interaction between docetaxel and SCO-101 in a docetaxel-resistant triple negative breast cancer cell line. Eur. J. Pharmaceutical Sci. 148:105315.

Norton L (1988) A Gompertzian model of human breast cancer growth. Cancer Res. 48(24, pt. 1):7067-7071.

O'Shaughnessy J, Blum J, Moiseyenko V, Jones SE, Miles D, Bell D, Rosso R, Mauriac L, Osterwalder B, Burger HU, Laws S (2001) Randomized, open-label, phase II trial of oral capecitabine (Xeloda[®]) vs. a reference arm of intravenous CMF as first-line therapy for advanced/metastatic breast cancer. *Ann. Oncolology* 12(9):1247–1254.

Palmeri L, Vaglica M, Palmeri S (2008) Weekly docetaxel in the treatment of metastatic breast cancer. *Therapeutics Clinical Risk Management* 4(5):1047–1059.

Panetta J, Adam J (1995) A mathematical model of cycle-specific chemotherapy. Math. Comput. Model. 22(2):67-82.

Pereira F, Pedreira C, De Sousa J (1995) A new optimization based approach to experimental combination chemotherapy. Frontiers Medical Biol. Engrg. 64(4):257–268.

Petrovski A, Sudha B, McCall J (2004) Optimising cancer chemotherapy using particle swarm optimisation and genetic algorithms. Yao X, Burke E, Lozano J, et al., eds. *Parallel Problem Solving from Nature—PPSN VIII* (Springer, Berlin/Heidelberg), 633–641.

Piraino S, Thomas V, O'Donovan P, Furney S (2019) Mutations: Driver vs. passenger. Boffetta P, Hainaut P, eds. *Encyclopedia of Cancer*, 3rd ed. (Academic Press, Oxford, UK), 551–562.

Pizzo P (1993) Management of fever in patients with cancer and treatment-induced neutropenia. New England J. Medicine 328:1323–1332.

Polyak K (2011) Heterogeneity in breast cancer. J. Clinical Investigation 121(10):3786-3788.

Reigner B, Blesch K, Weidekamm E (2001) Clinical pharmacokinetics of capecitabine. Clinical Pharmacokinetics 40(2):85-104.

Rosado M, Diamanti A, Cascioli S, Ceccarelli S, Caporuscio S, D'Amelio R, Carsetti R, Lagana B (2011) Hyper-IgM, neutropenia, mild infections and low response to polyclonal stimulation: Hyper-IgM syndrome or common variable immunodeficiency? *Internat. J. Immunopathology Pharmacology* 24(4):983–991.

Sager S (2005) Numerical Methods for Mixed-Integer Optimal Control Problems (Der Andere Verlag, Lübeck, Germany).

Saville C, Smith H, Bijak K (2019) Operational research techniques applied throughout cancer care services: A review. *Health Systems (Basing-stoke)* 8(1):52–73.

Senkus E, Kyriakides S, Ohno S, Penault-Llorca F, Poortmans P, Rutgers E, Zackrisson S, Cardoso F, ESMO Guidelines Committee (2015) Primary breast cancer: ESMO clinical practice guidelines for diagnosis, treatment, and follow-up. *Ann. Oncology* 26(suppl. 5):v8–v30.

Sharma R, Rivory L, Beale P, Ong S, Horvath L, Clarke SJ (2006) A phase II study of fixed-dose capecitabine and assessment of predictors of toxicity in patients with advanced/metastatic colorectal cancer. *British J. Cancer* 94(7):964–968.

Shi J, Alagoz O, Erenay F, Su Q (2014) A survey of optimization models on cancer chemotherapy treatment planning. *Ann. Oper. Res.* 221(1):331–356.

Skipper H, Schabel F Jr, Wilcox W (1964) Experimental evaluation of potential anticancer agents. XIII. On the criteria and kinetics associated with "curability" of experimental leukemia. Cancer Chemotherapy Rep. 35:1–111.

Skipper H, Schabel F Jr, Wilcox W (1967) Experimental evaluation of potential anticancer agents. XXI. Scheduling of arabinosylcytosine to take advantage of its S-phase specificity against leukemia cells. *Cancer Chemotherapy Rep.* 51(3):125–165.

Swan G, Vincent T (1977) Optimal control analysis in the chemotherapy of IgG multiple myeloma. Bull. Math. Biol. 39(3):317–337.

Swierniak A, Kimmel M, Smieja J (2009) Mathematical modeling as a tool for planning anticancer therapy. *Eur. J. Pharmacology* 625(1):108–121. Tan K, Khor E, Cai J, Heng C, Lee T (2002) Automating the drug scheduling of cancer chemotherapy via evolutionary computation. *Artificial Intelligence Medicine* 25(2):169–185.

Tan K, Li S, Li YR, Cheng S, Lin S, Tung Y (2019) Synergistic anticancer effect of a combination of paclitaxel and 5-demethylnobiletin against lung cancer cell line in vitro and in vivo. *Appl. Biochemistry Biotechnology* 187(4):1328–1343.

Tjørve K, Tjørve E (2017) The use of Gompertz models in growth analyses, and new Gompertz-model approach: An addition to the Unified-Richards family. *PLoS One* 12(6):1–17.

Tse S, Liang Y, Leung K, Lee K, Mok T (2007) A memetic algorithm for multiple-drug cancer chemotherapy schedule optimization. *IEEE Trans. Systems Man, Cybernetics Part B (Cybernetics)* 37(1):84–91.

Tyagi R, Dey P (2014) Needle tract seeding: An avoidable complication. Diagnostic Cytopathology 42(7):636–640.

Urquhart J, De Klerk E (1998) Contending paradigms for the interpretation of data on patient compliance with therapeutic drug regimens. Statist. Medicine 17(3):251–267.

Villasana M, Ochoa G (2004) Heuristic design of cancer chemotherapies. IEEE Trans. Evolutionary Comput. 8(6):513-521.

World Health Organization (1979) WHO Handbook for Reporting Results of Cancer Treatment (World Health Organization, Geneva, Switzerland). Wu Y, Zhang D, Wu B, Quan Y, Liu D, Li Y, Zhang X (2017) Synergistic activity of an antimetabolite drug and tyrosine kinase inhibitors against breast cancer cells. Chemical Pharmaceutical Bull. (Tokyo) 65(8):768–775.

Yang Q, Li M, Spiller OB, Andrey DO, Hinchliffe P, Li H, MacLean C, et al. (2017) Balancing mcr-1 expression and bacterial survival is a delicate equilibrium between essential cellular defence mechanisms. Nature Comm. 8(1):2054.

Yuan P, Di L, Zhang X, Yan M, Wan D, Li L, Zhang Y, et al. (2015) Efficacy of oral etoposide in pretreated metastatic breast cancer: A multi-center phase 2 study. *Medicine (Baltimore)* 94(17):e774.

Zietz S, Nicolini C (1979) Mathematical approaches to optimization of cancer chemotherapy. Bull. Math. Biol. 41(3):305-324.